CENTRUM TECHNIKI OKRĘTOWEJ

SHIP DESIGN AND RESEARCH CENTRE
ЦЕНТР СУДОСТРОИТЕЛЬНОЙ ТЕХНИКИ

zeszyty

PROBLEMOWE

REPORTS • ТРУДЫ

A. GALEWSKI, L. KONIECZNY

B – 006

COMPUTER CALCULATIONS OF SHIP HULL LONGITUDINAL STRENGTH WITH THE INTERACTION BETWEEN TORSION AND HORIZONTAL BENDING

GDAŃSK

SHIP DESIGN AND RESEARCH CENTRE

DIVISION OF SHIP STRUCTURE MECHANICS

B – 006

COMPUTER CALCULATIONS OF SHIP HULL LONGITUDINAL STRENGTH WITH THE INTERACTION BETWEEN TORSION AND HORIZONTAL BENDING

mgr inż. Andrzej Galewski, dr inż. Leszek Konieczny

BKD: 31032:31034:31025:30115

GDAŃSK, JUNE 1979

ABSTRACT

An algorithm of ship longitudinal strength calculation is given with the interaction between torsion and horizontal bending taken into account. The algorithm is based on the theory of thin walled beams and transfer matrix approach. A computer program, based on the presented algorithm, was worked out in Ship Design and Research Centre. Ship decks are idealized as plane frames and a whole flexibility matrix can be introduced to the data for each deck. Test results are given in the paper and some comparisons with experimental and FEM results are enclosed. Some practical results are also presented in the paper.

OBLICZENIA KOMPUTEROWE WYTRZYMAŁOŚCI OGÓLNEJ STATKU Z UWZGLĘDNIENIEM SPRZĘŻENIA SKRĘCANIA I ZGINANIA POPRZECZNEGO

Praca zawiera algorytm obliczeń wytrzymałości ogólnej kadłuba statku z uwzględnieniem sprzężenia skręcania i zginania poprzecznego. Algorytm ten opiera się na teorii belek cienkościennych i metodzie macierzy przejścia. Na bazie tego algorytmu opracowano w Centrum Techniki Okrętowej komputerowy program. Pokład statku otwartego traktowany jest jako rama płaska i w danych może być wprowadzona kompletna macierz podatności pokładu. W pracy podano wyniki obliczeń testowych wraz z porównaniem z wynikami obliczeń metodą elementów skończonych i z danymi eksperymentalnymi. Przedstawiono również niektóre przykłady zastosowań praktycznych programu.

КОМПЮТЕРНЫЕ РАСЧЕТЫ ОБЩЕЙ ПРОЧНОСТИ СУДНА С УЧЕТОМ СОПРЯЖЕНИЯ КРУЧЕНИЯ И ПОПЕРЕЧНОГО ИЗГИБА

Работа содержит алгоритм расчетов общей прочности корпуса судна с учётом сопряжения кручения и поперечного изгиба.
Алгоритм этот основан на теории тонкостенных стержней и методе матриц прохода. На базе этого алгоритма разработано в ЦТО компютерную программу. Открытая палуба судна принимается как плоская рама и в расчётные данные может быть введена комплектная матрица податливости палубы. В работе поданы результаты испытательных расчетов вместе с сопоставлением с результатами расчётов методом конечных элементов и с экспериментальными данными. Представлено также некоторые примеры практического применения программы.

CONTENTS

SPIS TREŚCI

СОДЕРЖАНИЕ

INTRODUCTION

The longitudinal strength of a ship hull has been so for examined mainly with respect to the bending in vertical plane, while horizontal bending and torsion are ignored. An additional analysis of torsion /considered as a separate problem/ has usually been performed only for open ships /e.g. for container ships/. However, as recent progress in practical calculations of the hydrodynamic wave pressures acting on the ship hull enables to determine the ship's structural response more exactly, an improved longitudinal strength calculation procedure, including horizontal bending and torsion effects, is more and more needed. The longitudinal strength analysis, with horizontal bending and torsion taken into account, is a rather difficult task because of the complex hull shape. . Though the finite element method /FEM/ provides exact results, it requires enormous labour and cost, so it is unsuitable for the initial desing calculations of a total ship structure. Therefore this paper deals with an approximate method based on the thin-walled beam theory.

However, this approach requires a lot of problems to be carefully considered. First task to be solved is how to handle a thin-walled hull structure having a variable cross section and structural discontinuities at bulkheads, as well as bulky cross decks at bow, stern and engine room. The effect of the coupling of hull bending in horizontal plane and torsion is to be considered, because the shear centres of the hull cross sections are not aligned. The determination of the member properties /like shear and torsional rigidity/ requires intricate calculations due to complex cross section of the ship hull.

Numerous papers on the torsional strength of container ships have been published dealing with the above mentioned problems. All of them consider the ship torsion as a separate problem without regard to the coupling effects. Among them, mention should be made of the important paper by K. Haslum et al [3] who solved the problem of torsion of thin-walled beams with a variable cross section and section discontinuities applying the thin-walled beam theory according to the Kollbrunner and Hajdin formulation [1], [2] and the transfer matrix method. However, the comparison with the results of the FEM calculations [7], [8] performed later, has revealed some significant inaccuracies in the Haslum's algorithm, even in the case of a simple torsion load. In the case of complex loading, when bending and torsion occur simultaneously, it is necessary to

consider the coupling between torsion and horizontal bending.

S. Shimizu et. al. [4] published an algorithm of the longitudinal strength calculation with coupling between torsion and horizontal bending taken into account. The algorithm is also based on the thin-walled beam theory and transfer matrix method, but there are coupling terms in the cross section transfer matrices taking the coupling effects between torsion and horizontal bending into account.

The algorithm of the longitudinal strength calculation presented in this paper is similar to that worked out by Shimizu et al. [4]. However, segment transfer matrices are developed with additional warping due to the warping shear stresses according to the K lbrunner and Hajdin formulation [2] and particular integrals of the differential equations of hull torsion and bending have been found for the most general load /trapezoidal distribution of load acting on any part of the hull segment/ instead of the trapezoidal distribution over the whole segment length, as it is assumed in [4].

A computer program, based on the presented algorithm, was worked out in The Ship Design and Research Centre, special attention having been paid to the effect of the transverse and longitudinal deck strips on the torsional response of an open ship. Ship decks are idealized as plane frames and a whole flexibility matrix can be introduced to the data for each deck. In such a way the effect of local bending of a deck can more exactly be taken into account than it would be possible by considering the transverse deck strips as isolated beams, as it is usually done e.g. in [3], [4].

The computer results were thoroughly investigated and some comparisons with experimental and FEM results enclosed /example A and B/. Some improvements have been introduced in the coupling term in cross section transfer matrices and appropriate results tested. Some practical results are also presented in the paper /example C and D/. The suggested field of the program application as well as the research areas are given in the conclusions.

INDEX OF SYMBOLS

l	- length of a beam
m_D	- external torque intensity /about shear centre D/
m_x, m_y	- external bending moment intensity
m_Ω	- external bimoment intensity
p_x, p_y, p_z	- external load intensity acting over a line
s	- curvilinear coordinate of the middle surface
t	- wall thickness
u	- displacement normal to the middle surface
v	- displacement tangential to the middle surface
w	- axial displacement
x, y	- cartesian coordinates in the principal directions of the cross section
z	- longitudinal coordinate
G	- centre of gravity
D	- shear centre
E	- modulus of elasticity
F	- cross section area
$\tilde{F}$	- area of the considered part of the cross section /from the stress-free edge to any point s where the shear stress is wanted/
G	- shear modulus
$I_{xx} = \int_F x^2 dF$	- moment of inertia
$I_{yy} = \int_F y^2 dF$	- moment od inertia
$I_{x,y} = \int_F xy dF$	- deviation moment
$I_{\omega\omega P} = \int_F \omega^2 dF$	- sectorial moment of inertia about any pole P
$I_{\Omega\Omega} = \int_F \Omega^2 dF$	- sectorial moment od inertia for normalized sectorial coordinates
$I_{x\omega P} = \int_F \omega_P x dF$	- sectorial deviation moment
$I_{y\omega P} = \int_F \omega_P y dF$	- sectorial deviation moment
K	- St.Venant torsional moment of inertia
$M_x = \int_F \sigma x dF$	- bending moment

$M_y = \int \sigma_y \, dF$ - bending moment

$M_\Omega = \int \sigma \Omega \, dF$ - bimoment

$\bar{M}_\Omega$ - external bimoment

N - axial force

0 - zero point for s coordinate

Q_x, Q_y - shear force acting in x and y direction

$\bar{Q}_x, \bar{Q}_y$ - external point loads acting in x and y direction

$S_{\omega P} = \int_F \omega_P \, dF$ - static sectorial moment

$\tilde{S}_x = \int_F x \, dF$
$\tilde{S}_y = \int_F y \, dF$ - static moment of the considered part $\tilde{F}$ of the cross section

$\tilde{S}_\Omega = \int_F \Omega \, dF$ - sectorial static moment of the considered part $\tilde{F}$ of the cross section

T - torsional moment about the shear centre

$\bar{T}$ - external torsional moment

T_S - St.Venant torsional moment

$T_{\omega P}, T_\Omega$ - warping torsional moment

$\gamma_{z,s}$ - shear deformation

$\varepsilon_z, \varepsilon_y, \varepsilon_n$ - linear deformations

σ - axial /normal/ stress

τ_s - St.Venant shear stress

τ_w - warping shear stress

φ - rotational angle

$\varphi' = \frac{dy}{dz}$ - slope of angle /twisting rate/

Ω - unit warping /normalized sectorial coordinate/

q - shear flow

$q_s = t\tau s$ - shear flow for St.Venant torsion

$q_w = t\tau w$ - shear flow for warping torsion

v - warping factor

$\rho = \frac{I_{hh}}{I_{hh} - K}$

l_n - length of the element number n

e_n - shear centre coordinate for element number n

c_n - centre of gravity coordinate for the element number n

D - ship depth

χ - angle of cross section rotation in $y\,z$ plane

ψ - angle of cross section rotation in $x\,z$ plane

ξ, η, ζ - displacements of shear centre in $x\,y\,z$ direction

$A_x^{(n)}$ - cross section shear area in $x\,z$ plane for the element number n

$A_y^{(n)}$ - cross section shear area in $y\,z$ plane for the element number n

1. APPLICATION OF THE TRANSFER MATRIX METHOD TO SHIP'S LONGITUDINAL STRENGTH CALCULATIONS

The ship hull is assumed to be a thin-walled beam with variable cross-section, represented by a number of elements with constant cross-section, as it is shown in Fig. 1. After assuming kinematic and static compatibility between elements /i.e. a cross-section transfer matrix/, appropriate differential equations for any element are solved in a similar way as for the prismatic beam where the element transfer matrix is easy to determine. The transfer matrix method is well suited for computer calculations of the longitudinal ship strength.

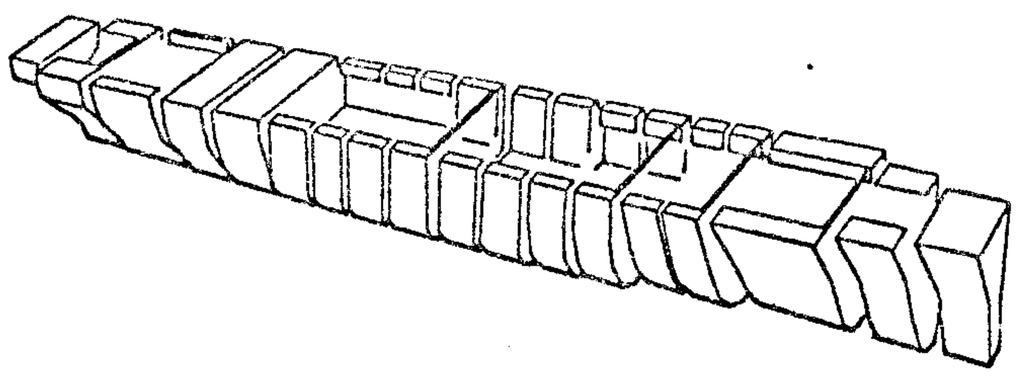

Fig. 1. An idealization of the ship hull in the transfer matrix method

It is further assumed that the ship hull has the longitudinal plane of symmetry i.e. diametral plane. As a result bending in vertical plane can be considered independently, but torsion and bending in horizontal plane are coupled /because the cross section shear centres are not aligned/.

In deriving an element transfer matrix it is assumed that the centre of gravity G is chosen as the origin of the x, y coordinate system, the element displacements are, however, determined in relation to the shear centre D which constitutes the rotation centre of the element /Fig. 2/. External loads are reduced to the cross section shear centre, so torsion of an element can be considered as independent of bending. Assuming the sign convention as in Fig. 2 /the positive clockwise angle of rotation when looking in the positive z direction/, one can obtain the following expressions[x/] for the displacements and stress resultants /shear deformation included/

---

x/ for the notation used in the paper see index of symbols enclosed

$$M_x = EI_{xx}^{(n)} \frac{d\psi}{dz}$$

$$M_y = EI_{yy}^{(n)} \frac{d\chi}{dz}$$

$$Q_x = GA_x^{(n)} \left(\frac{d\xi}{dz} - \psi\right)$$

$$Q_y = GA^{(n)} \left(\frac{d\eta}{dz} - \chi\right) \qquad /1a\text{–}g/$$

$$T_S = GK^{(n)} \frac{d\varphi}{dz}$$

$$T_\Omega = -\rho_n EI_{\Omega\Omega}^{(n)} \frac{d^3\varphi}{dz^3} - \frac{1}{k_{I,n}^2} \frac{dm}{dz}$$

$$M_\Omega = -\rho_n EI_{\Omega\Omega}^{(n)} \frac{d^2\varphi}{dz^2} - \frac{m}{k_{I,n}^2}$$

Where:

$EI_{xx}^{(n)}$ - bending stiffness in x, z plane

$EI_{yy}^{(n)}$ - bending stiffness in y, z plane

$GA_x^{(n)}$ - shear stiffness in x, z plane

$GA_y^{(n)}$ - shear stiffness in y, z plane

$GK^{(n)}$ - St. Venant torsion stiffness

$\rho_n EI_{\Omega\Omega}^{(n)}$ - warping torsion stiffness

$$K_{I,n}^2 = \frac{GI_{hh}^{(n)}}{\rho_n EI_{\Omega\Omega}^{(n)}} \quad ; \quad \rho_n = \frac{I_{hh}^{(n)}}{I_{hh}^{(n)} - K^{(n)}}$$

The most general load (p_x , p_y , p_D) distribution is assumed as a trapezoidal distribution along any part of the element n of the hull girder /Fig. 3/.

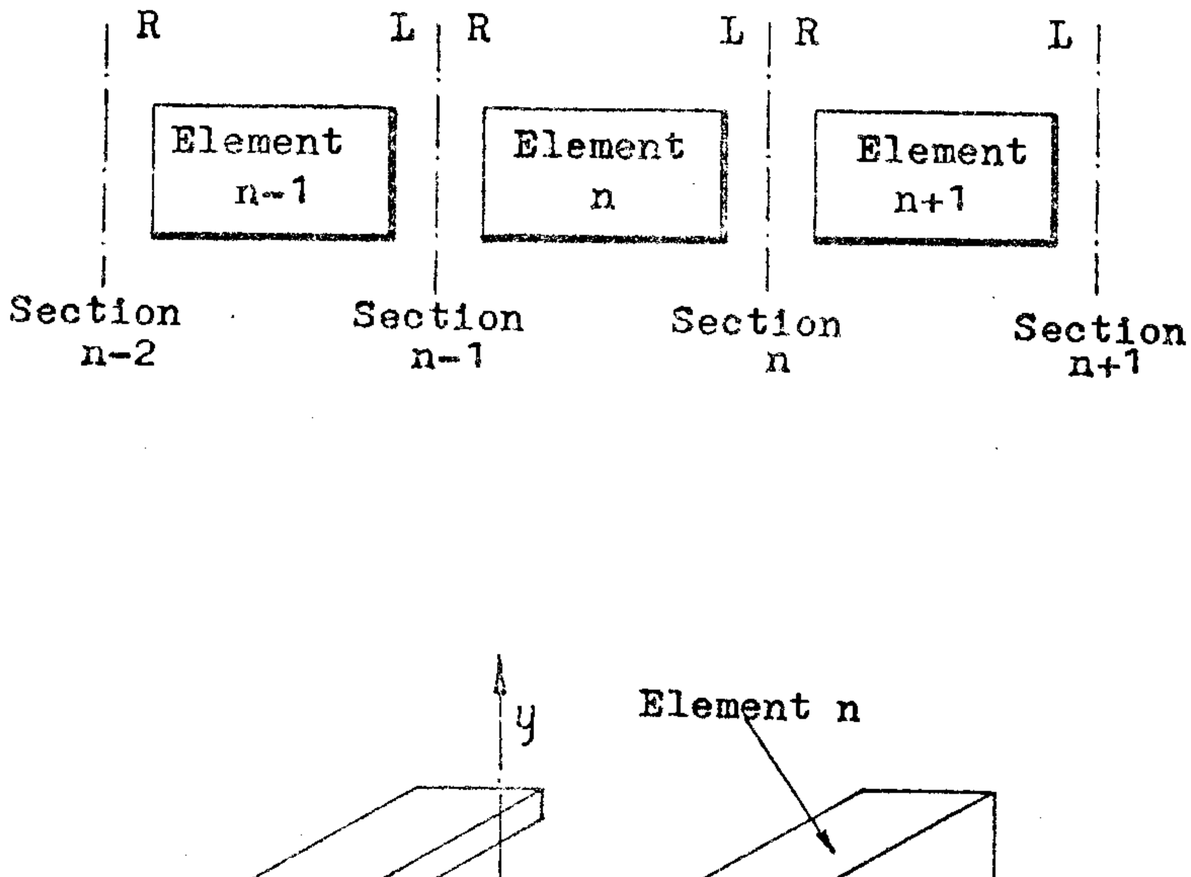

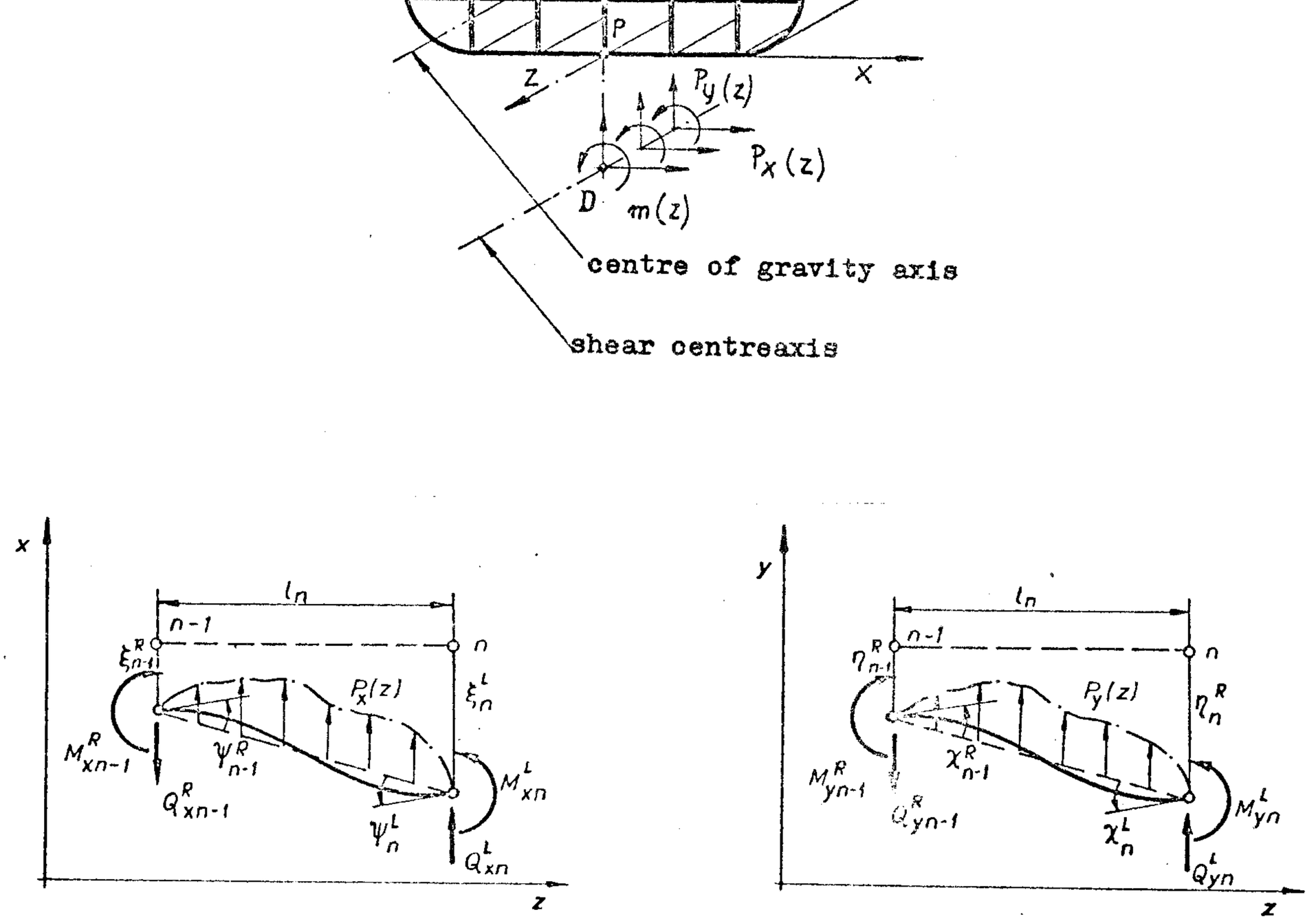

Fig. 2. Coordinate system and sign convention

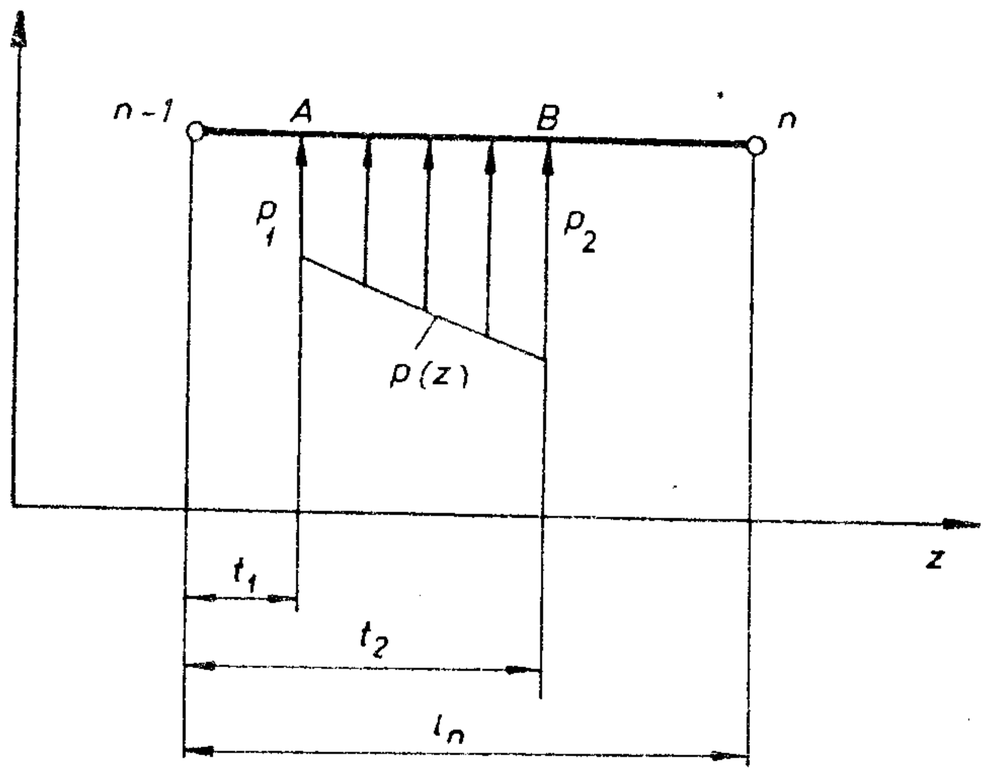

Fig. 3. Load distribution

Relation between state vectors /i.e. displacements and stress resultants of the hull girder/ at the end cross sections of the element number n is derived in the following nondimensional form

$$\mathbb{X}_n^L = \mathbb{F}_n \mathbb{X}_{n-1}^R \qquad /2/$$

where $\mathbb{F}_n$ denotes a nondimensional transfer matrix of the element number n

$$\mathbb{F}_n = \begin{bmatrix} K_y & 0 & 0 & k_y \\ 0 & K_x & 0 & k_x \\ 0 & 0 & K_\varphi & k_\varphi \\ 0 & 0 & 0 & 1 \end{bmatrix}_n \qquad /3/$$

State vectors connected with the cross section number n, can be also introduced in the nondimensional form

$$\mathbb{X}_{n-1}^R = \left\{ \mathbb{X}^1, \mathbb{X}^2, \mathbb{X}^3, 1 \right\}_{n-1}^R$$
$$\mathbb{X}_n^L = \left\{ \mathbb{X}^1, \mathbb{X}^2, \mathbb{X}^3, 1 \right\}_n^L \qquad /4a\text{-}b/$$

$$\mathbb{X}^1 = \left\{ \frac{\eta}{b^*}, \chi, \frac{b^* M_y}{E I_{yy}^*}, \frac{Q_y}{G A_y^*} \right\}$$
$$\mathbb{X}^2 = \left\{ \frac{\xi}{b^*}, \psi, \frac{b^* M_x}{E I_{xx}^*}, \frac{Q_x}{G A_x^*} \right\} \qquad /5a\text{-}c/$$
$$\mathbb{X}^3 = \left\{ \varphi, b^* v, \frac{M_\Omega}{G k^*}, \frac{b^* T}{G k^*} \right\}$$

Properties of the midship cross section are denoted with asterisk (*) in the above expressions where b^* represents the width of the midship cross section on the upper deck level. The indices R and L denote, respectively, the right and left hand side of the cross section number n at the boundary between the element number $(n-1)$ and n . The contents of the matrix $\mathbb{F}_n$ is given in Appendix A.

The compatibility condition of displacements and the equilibrium condition of stress resultants at the boundary between elements hold in relation to any reference axis, common for the whole hull girder. The following conditions hold for the reference axis going through the point P on the hull base plane /Fig. 2/.

$$\xi^R_{P,n} = \xi^L_{P,n}$$

$$M^R_{\omega P,n} = M^L_{\omega P,n} \quad \text{where } M_{\omega P} = \int_F \omega_P \sigma \, dF$$

$$T^R_{P,n} = T^L_{P,n}$$

They couple displacements and stress resultants at the right and left hand sides of the section number n. The above conditions can be transformed to the more specific expressions.

$$\xi^R_n = \xi^L_n - \varphi^L_n (e_{n+1} - e_n)$$

$$M^R_{\Omega,n} = M^L_{\Omega,n} - M^L_{x,n}(e_{n+1} - e_n) \qquad /6a\text{-}c/$$

$$T^R_n = T^L_n + Q^L_{x,n}(e_{n+1} - e_n)$$

if appropriate transformation rules for displacements and sectorial coordinates are taken into account /Appendix B/.

Index R denotes the response parameters of the element $(n+1)$ determined in relation to the shear centre of this element at its left end. Index L denotes the response parameters of the element n determined in relation to the shear centre of this element at its right end.

If cross section shape at the left and right hand side of the considered section differs completely, as it is shown in Fig. 4, the sectorial coordinates /unit warping $\Omega(s)$ / will have different distribution and magnitude for both sections.

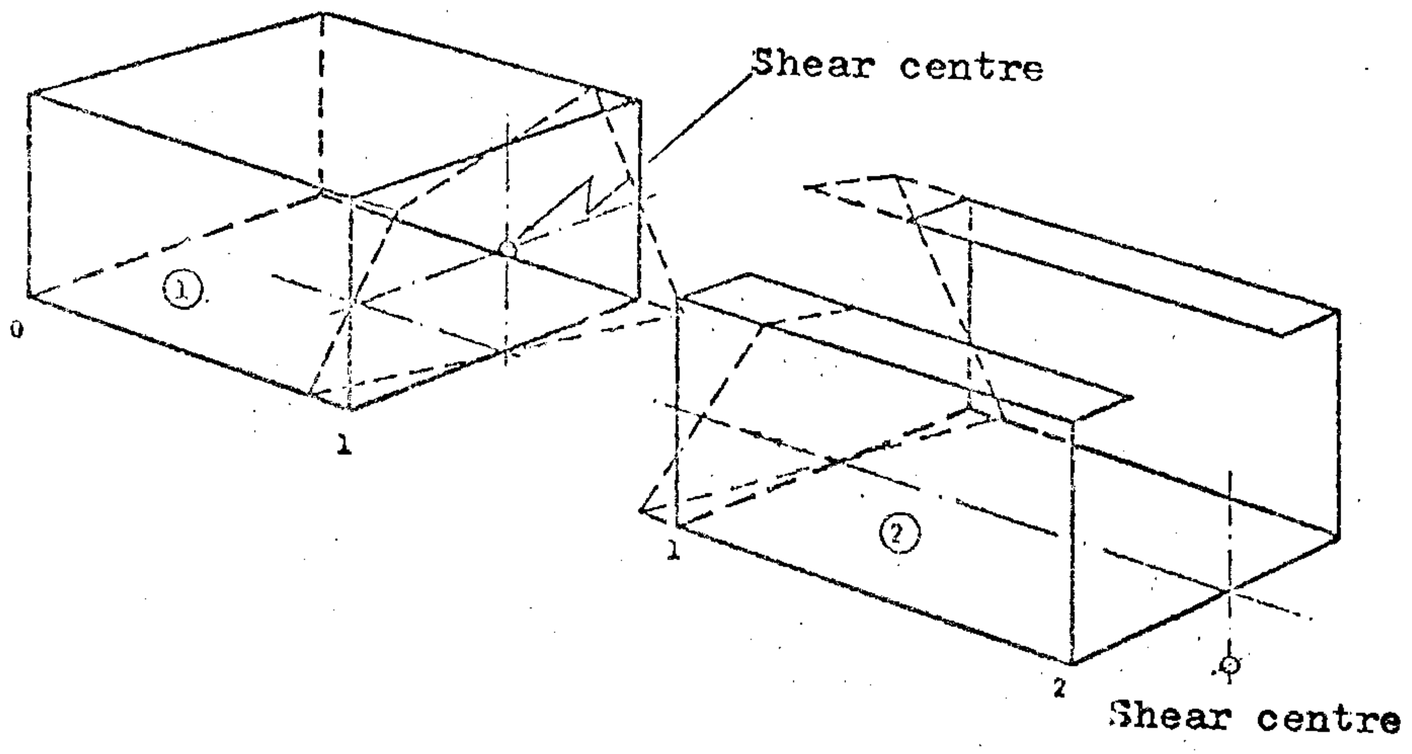

Fig. 4. Warping of cross sections with completely different shapes
different shapes

To obtain the best possible overall compatibility of longitudinal displacements it is assumed according to Haslum et al. [3] that the warping factor function $v(z)$ may be discontinuous at $z = z_1$

$$v(z_1^+) = \alpha\, v(z_1^-) \qquad /7/$$

The scalar α is called "warping compatibility factor".

The distribution of normal /warping/ stresses over a cross section is similar to the warping itself. Statical compatibility of stresses in every single point along the profile can not be achieved at $z = z_1$. However, the condition of overall internal equilibrium implies equality of the virtual work performed by stresses on the two cross sections under a virtual displacement e.g. $\bar{v}(z_1)$ It follows that bimoment function $M_\Omega(z)$ is also discontinuous at $z = z_1$ i.e.

$$M_\Omega(z_1^+) = \frac{1}{\alpha}\, M_\Omega(z_1^-) \qquad /8/$$

A good first approximation to α is derived by Haslum et al. [3].

$$\alpha \cong \sqrt{\frac{I_{\Omega\Omega}(z_1^-)}{I_{\Omega\Omega}(z_1^+)}} \qquad /9/$$

In conclusion, the compatibility conditions at cross section between elements n and $(n+1)$ can be derived in the following form

$$\xi_n^R = \xi_n^L - \varphi_n^L (e_{n+1} - e_n)$$

$$\psi_n^R = \psi_n^L$$

$$M_{x,n}^R = M_{x,n}^L$$

$$Q_{x,n}^R = Q_{x,n}^L - \bar{Q}_{x,n}$$

$$\varphi_n^R = \varphi_n^L \qquad /10a\text{-}h/$$

$$\upsilon_n^R = \alpha_n \upsilon_n^L$$

$$M_{\Omega,n}^R = \frac{1}{\alpha_n} M_{\Omega,n}^L - M_{x,n}^L (e_{n+1} - e_n) - \bar{M}_{\Omega,n}$$

$$T_n^R = T_n^L + Q_{x,n}^L (e_{n+1} - e_n) - \bar{T}_n$$

where $\bar{Q}_{x,n}$, $\bar{M}_{\Omega,n}$, $\bar{T}_n$ denote positive external loads applied at section n.

A warping factor υ occurs in the above expressions instead of a torsional angle slope φ' as it is in the expressions derived by Shimizu et al.[4]. Horizontal displacements ξ of element shear centres will occur /due to 10a/ even if there is no horizontal bending moment ($M_x = 0$). In the opposite case i.e. if horizontal bending takes place ($M_x \neq 0$) cross section rotations will occur /due to 10g/, even in the case of no torsional load ($T = 0$). Compatibility and equilibrum conditions /10/ can be represented in a nondimensional matrix form

$$\mathbb{X}_n^R = \mathbb{P}_n \mathbb{X}_n^L \qquad /11/$$

To derive the transfer matrix for the whole hull girder we denote $\mathbb{X}_A = \mathbb{X}_0^R$ a state vector composed of stress resultants and displacements at the stern and $\mathbb{X}_F = \mathbb{X}_N^L$ a state vector at the bow /N equal to the number of elements/. Applying the conventional transfer matrix procedure we obtain

$$\mathbb{X}_N^L = \mathbb{F}_N \{ \mathbb{P}_{N-1} \mathbb{F}_{N-1} \} \cdots \{ \mathbb{P}_2 \mathbb{F}_2 \} \{ \mathbb{P}_1 \mathbb{F}_1 \} \mathbb{X}_0^R$$

or in a short form

$$\mathbb{X}_F = \mathbb{F}\,\mathbb{X}_A \qquad /12/$$

where

$$\mathbb{F} = \mathbb{F}_N \left\{ \mathbb{P}_{N-1}\, \mathbb{F}_{N-1} \right\} \cdots \left\{ \mathbb{P}_2 \mathbb{F}_2 \right\} \left\{ \mathbb{P}_1\, \mathbb{F}_1 \right\} \qquad /13/$$

is the transfer matrix for the whole hull girder. Now it is possible to determine state vectors at stern $\mathbb{X}_F$ and bow $\mathbb{X}_A$ from equation /12/ and from the boundary conditions. Displacements and stress resultants at any cross section of an element number i can be determined through the following procedure

$$\mathbb{X}_i^L(z) = \mathbb{F}_i(z) \left\{ \mathbb{P}_{i-1}\, \mathbb{F}_{i-1} \right\} \cdots \left\{ \mathbb{P}_2\, \mathbb{F}_2 \right\} \left\{ \mathbb{P}_1\, \mathbb{F}_1 \right\} \mathbb{X}_A \qquad /14/$$

2. GENERAL DESCRIPTION OF THE COMPUTER PROGRAM

The algorithm described above can effectively be applied only on a large computer. A program based on this algorithm was worked out in the Ship Design and Research Centre in Gdańsk. The program /running on an ICL 4-70 computer/ consists of 6250 cards and occupies 180 000 bytes of the core store. All calculations are performed in the double precision and an overlay technique is effectively applied.

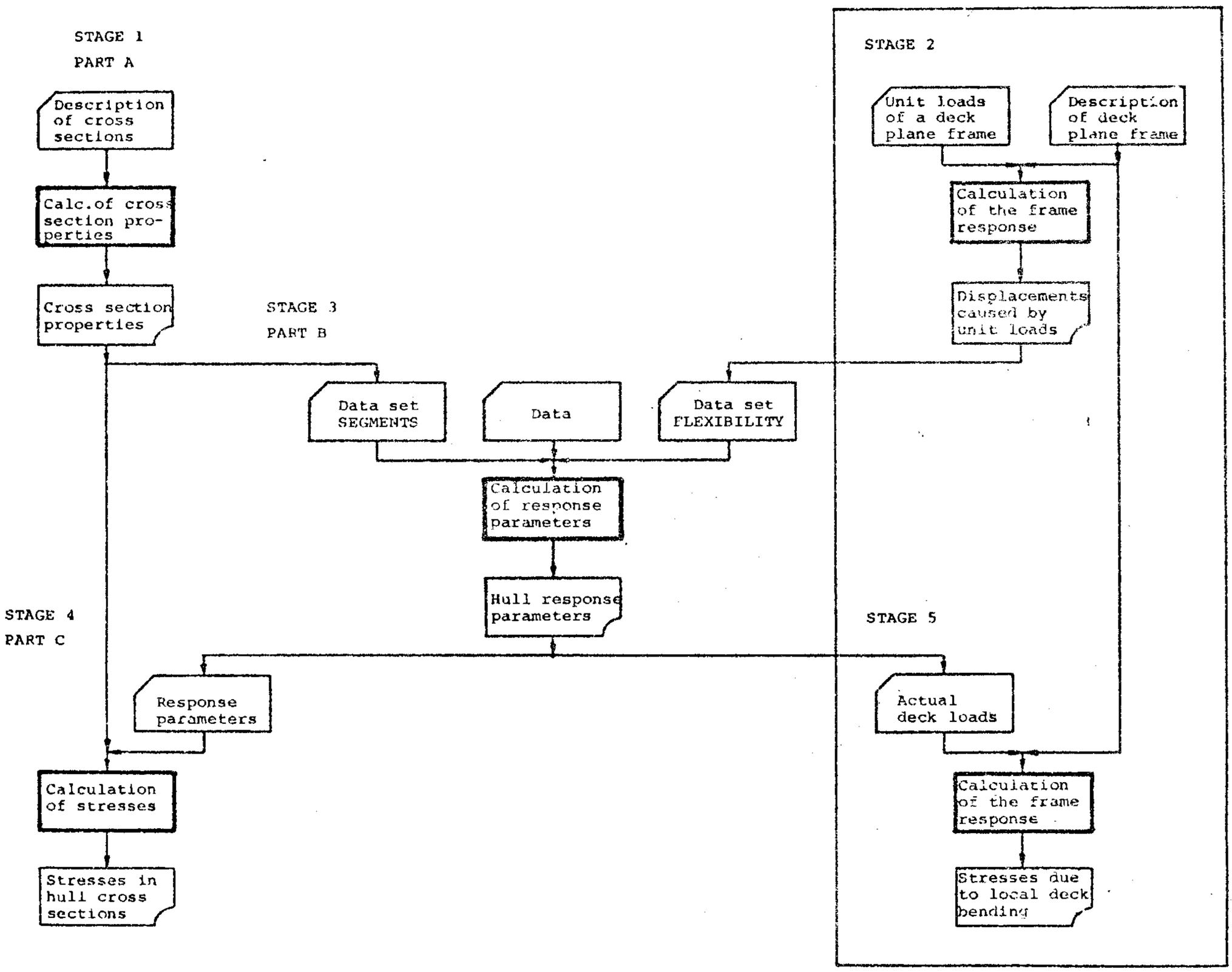

Fig. 5. Flow chart of the program application

The program enables to determine hull stresses and deformations, as well as additional stresses due to the local bending of deck caused by the hull torsion and consists of the following stages:

1/ Calculation of cross section properties;

2/ Calculation of plane frame deformations /for every deck/ caused by unit loads, to determine the flexibility matrices of decks;

3/ Calculation of ship's hull response parameters caused by an actual external load;

4/ Calculation of stresses and strains in the cross sections of the hull;

5/ Calculation of additional stresses due to the local bending of the deck structure caused by the hull torsion.

The program makes it possible to perform directly the stages 1,3 and 4 by the part A, B and C of the program, respectively. Mention should be made that it is possible to determine stresses and deformations /due to hull bending and torsion/ in a single run, providing the cross sections properties are given. Stages 2 and 5 are, however, to be performed using a separate program for the plane frame analysis.

At the program development special attention was paid to the effect of the transverse and longitudinal deck strips on the torsional response of open ships. The ships with large hatch openings have at least some reinforced transverse deck strips fitted, located between the open parts /Fig.6a/. The force method approach, similar to the one used in [10], was applied to find out the beneficial influence of the transverses.

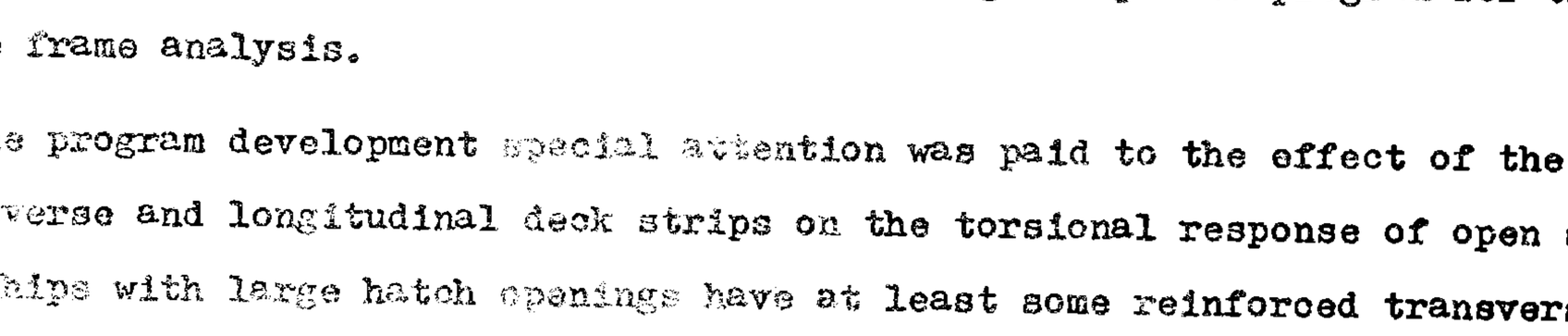

Fig. 6. An equivalent isostatic system for transverse deck strips

The actual system is replaced by an equivalent isostatic one, obtained through cutting of each transverse at the midpoint /Fig.6b/. However, the redundant shear forces $Z_1, Z_2 \dots Z_n$ are introduced to nullify the relative displacement of the two disconnected edges. The following system of equations represent the appropriate compatibility conditions in the case of N transverse strips

$$
\begin{aligned}
(\delta_{11} + \bar{\delta}_{11}) Z_1 + (\delta_{12} + \bar{\delta}_{12}) Z_2 + \dots + (\delta_{1N} + \bar{\delta}_{1N}) Z_N &= \Delta_1 \\
(\delta_{21} + \bar{\delta}_{21}) Z_1 + (\delta_{22} + \bar{\delta}_{22}) Z_2 + \dots + (\delta_{2N} + \bar{\delta}_{2N}) Z_N &= \Delta_2 \\
\dots\dots\dots\dots\dots\dots\dots\dots\dots\dots\dots\dots & \\
(\delta_{N1} + \bar{\delta}_{N2}) Z_1 + (\delta_{N2} + \bar{\delta}_{N2}) Z_2 + \dots + (\delta_{NN} + \bar{\delta}_{NN}) Z_N &= \Delta_N
\end{aligned}
\qquad /15/
$$

When the redundant shear forces $Z_i \ (i = 1, 2 \dots n)$ are determined it is possible to calculate bimoments that replace the transverse strips action in the equivalent isostatic system. The transfer matrix method procedure, described in the previous section, should be applied for the simultaneous action of the external loading and the bimoments.

Both the coefficients and free terms of the equations /15/ have physical meaning of relative displacements of the disconnected edges of the deck transverse strips. While Δ_i and δ_{ij} mean relative displacements of the disconnected edges of the undeformable transverse deck strips /Fig. 7/, caused by the external load and the unit shear force Z_i, respectively, coefficients $\bar{\delta}_{ij}$ describe full flexibility properties connected with the local bending of the deck structure. In order to determine the flexibility coefficients $\bar{\delta}_{ij}$ a plane frame analysis is to be performed with shear deformations of members taken into account /Fig. 8/. When the redundant shear forces Z_1 are determined, after solution of the equations /15/, additional stresses due to the local bending can easily be found from the deck plane frame analysis.

Main advantage of the presented approach /see [9] / is that full coefficient matrix $[\bar{\delta}_{ij}]$ is taken into account, instead of only diagonal terms, as it is usually done /in [10], for instance/.

Using the program it is possible to take also longitudinal deck strips into account. In this case, however, the equivalent isostatic system becomes far more complicated, as the degree of redundancy increases, even if only the axial stiffness of the longitudinal deck strips is regarded /the bending and shear stiffness being neglected/.

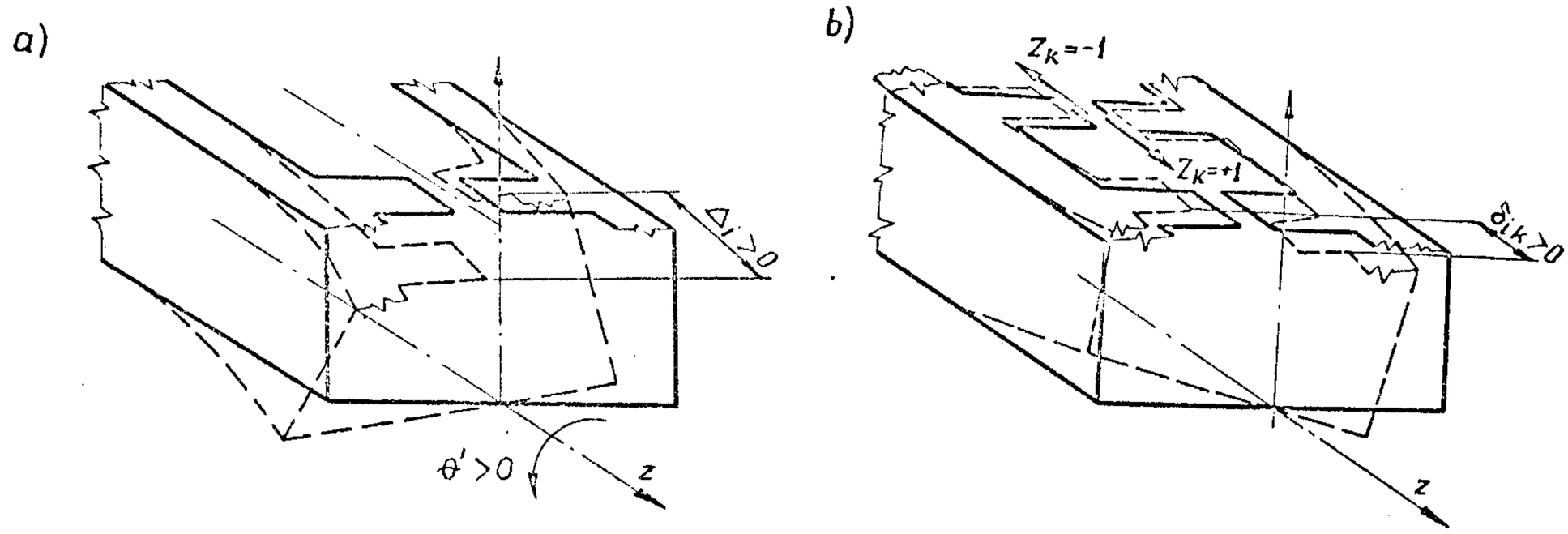

Fig. 7. Relative displacement of disconnected strip edges for the undeformable deck strips

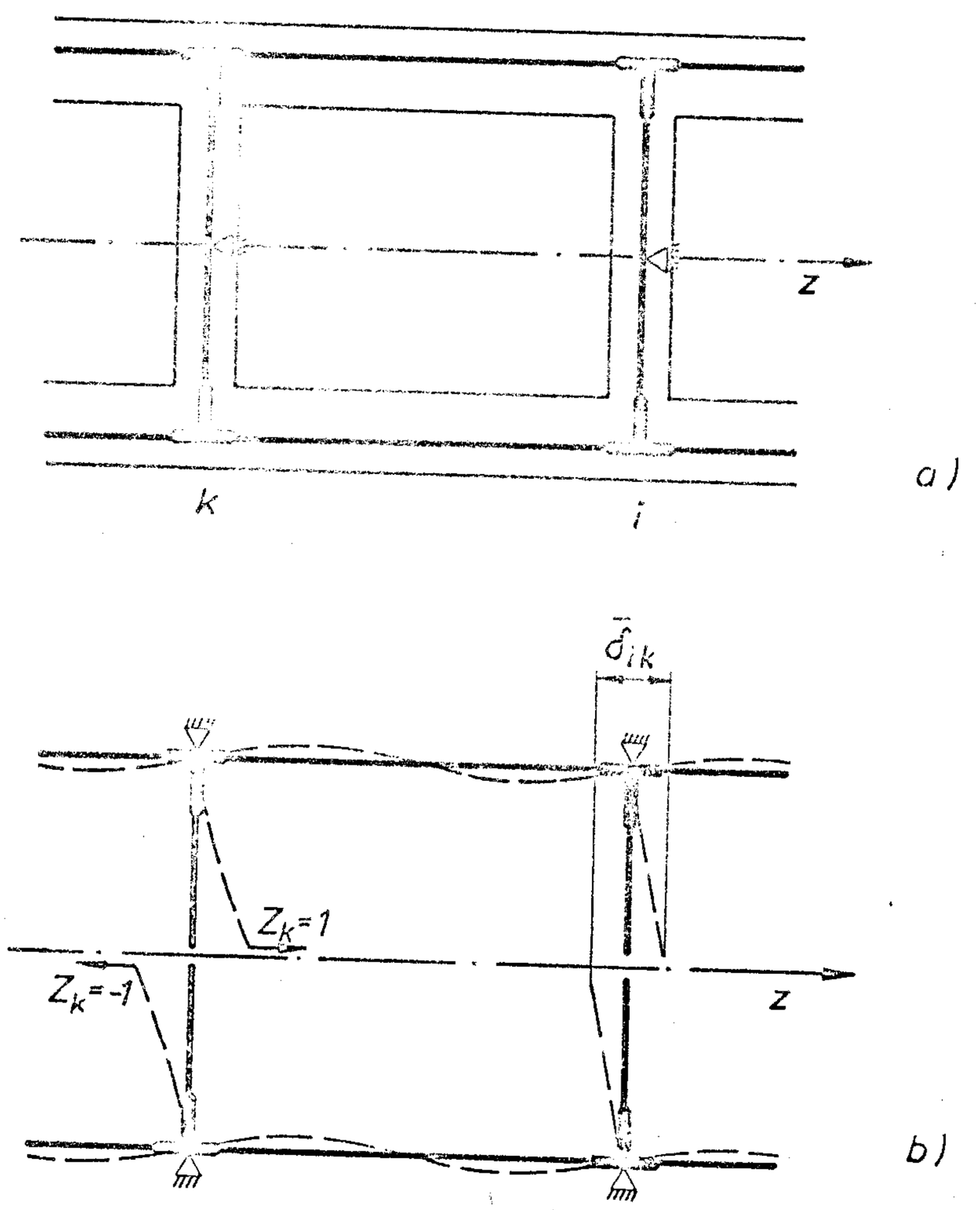

Fig. 8. Relative displacements $\bar{\delta}_{ij}$ due to the local bending of a deck structure

3. EXAMPLE A. A THIN-WALLED BEAM WITH CONTINUOUSLY VARIABLE OPEN CROSS SECTION

Torsion of a thin-walled beam shown in Fig. 9 is considered as the first example of the program application. The beam has channel cross sections with flange width varying according to the parabola rule. It is clamped at both ends and loaded by a torsional moment acting at the middle section /i.e. in the symmetry plane of the beam/.

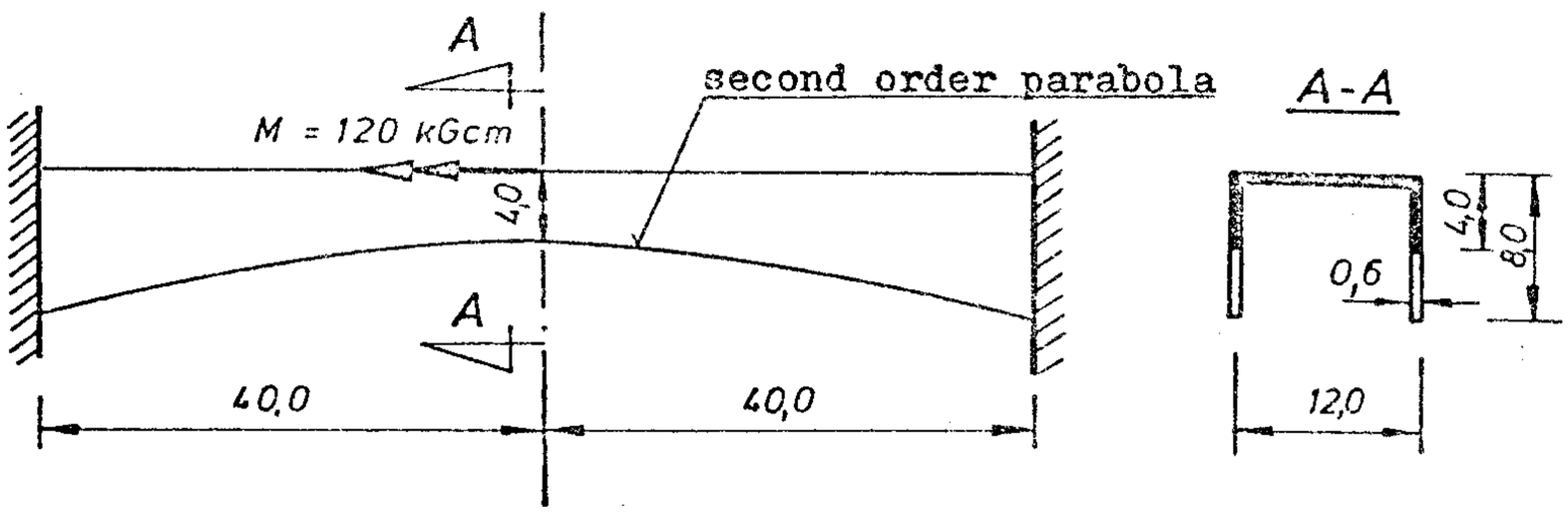

Fig. 9. A channel beam, clamped at both ends, loaded by a concentrated torsional moment

The choice of the beam was intentional as it is the only test example of a thin-walled beam with continuously variable cross section the authors have found in the literature. The problem had been solved using various numerical methods /finite difference, finite element method/ and the results compared with an experiment [6].

Calculations, based on the thin-walled beam theory and transfer matrix method, were performed using the computer program described above. Particular attention was paid to the accuracy of results as dependent on the way of idealization. Computed results were compared with the experimental data according to [6]. Angles of rotation and warping /normal/ stresses, determined by the experiment, are marked with circles in Fig. 10 and 11.

Computed rotation angles in the case of half-length of the beam divided into 5 and 10 elements with constant cross section are marked with full line in Fig. 10. These results were obtained after assuming $\rho = 1$ and $\alpha = 1$.

The assumption $\rho=1$ means that the warping due to the warping shear stresses is omitted, as it is usually done in the theory of thin-walled beams with open cross sections. The assumption $\alpha=1$ means that fictitious discontinuity at cross sections between elements is disregarded. Cross section properties /constant over an element length/ are assumed as the mean of the values at the element ends. Computed rotation angles, when ρ is calculated according to the "exact" formula given on the page 11, are marked with dashed lines in Fig. 10. For an open cross section the magnitude of the coefficient ρ tends asymptotically to 1 when the ratio of the cross section dimension to the wall thickness tends to infinity. In the case under consideration the ρ values range from 1.006 to 1.008. Computed rotation angles for the fictitious discontinuity at cross sections between elements taken into account are drawn with dot-and-dash line. Warping compatibility coefficient at these cross sections was determined according to the formula /9/.

The computed results obtained for $\rho=1$ and $\alpha=1$ /full line diagrams/ coincide well with the experimental data. The results obtained for 10 element partition differ very little from those related to 5 element partition. It should be stressed, however, that the results for 5 element discretization are closer to the experimental data than those for 10 element partition. It is probably a consequence of the transfer matrix method itself, where a beam with the continuously variable cross section is idealized as the one with stepwise variable cross section properties. When the number of beam elements rises, the transfer matrix method solution will not tend to the exact solution but to an approximate one. Therefore it can happen that the solution obtained for a coarse discretization is more exact than the solution related with a finer subdivision, as it is the case in the considered example.

The allowance for fictitious discontinuity at cross sections between elements, made through introducing α determined according to /9/, leads to significant inaccuracies. It is therefore recommended to put $\alpha=1$ at these sections. Likewise, $\rho=1$ should be assumed instead of the "exact" ρ value according to the formula given on page 11 when a beam with an open cross section is considered.

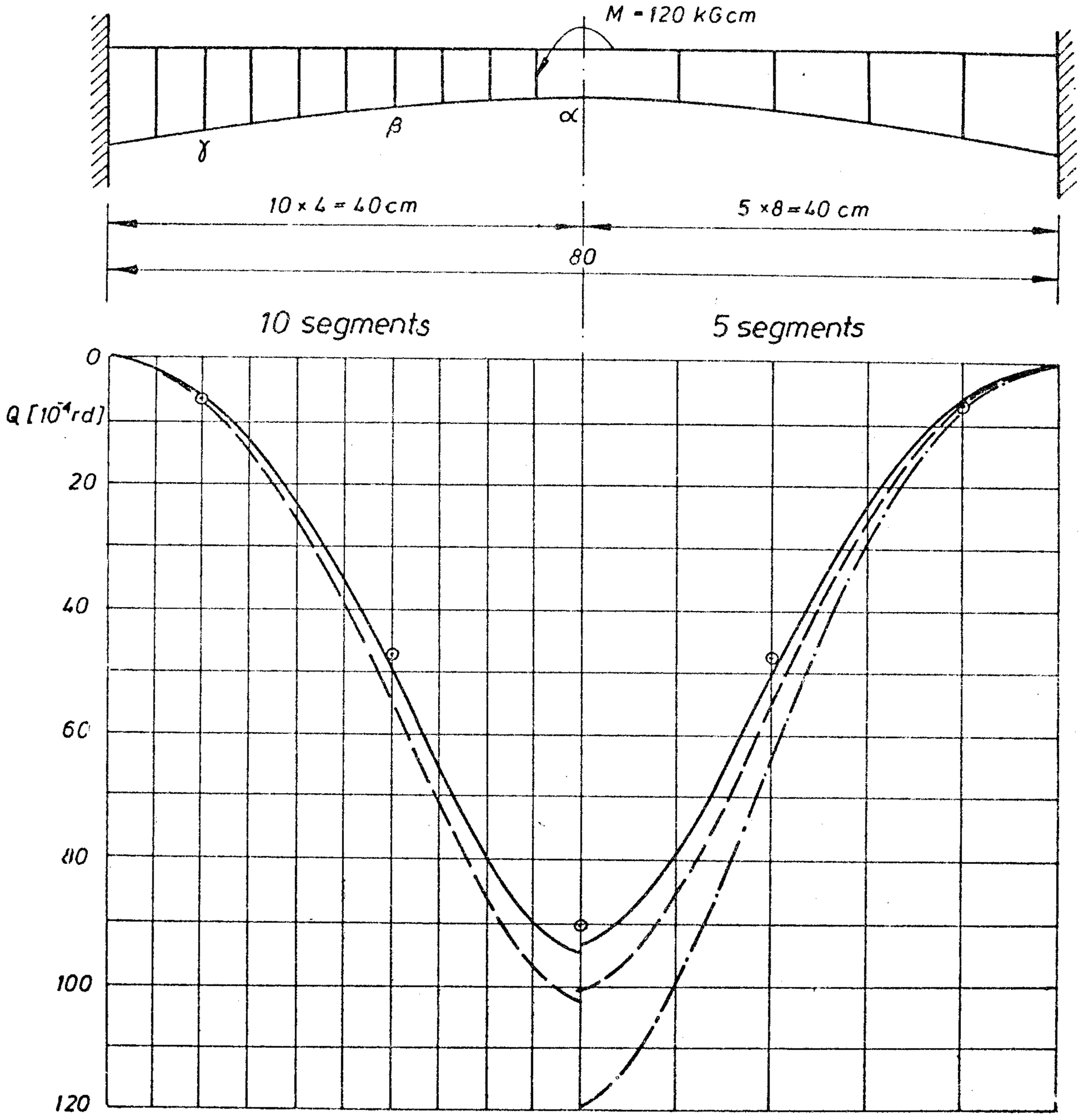

Fig. 10. Rotation angles of the channel beam

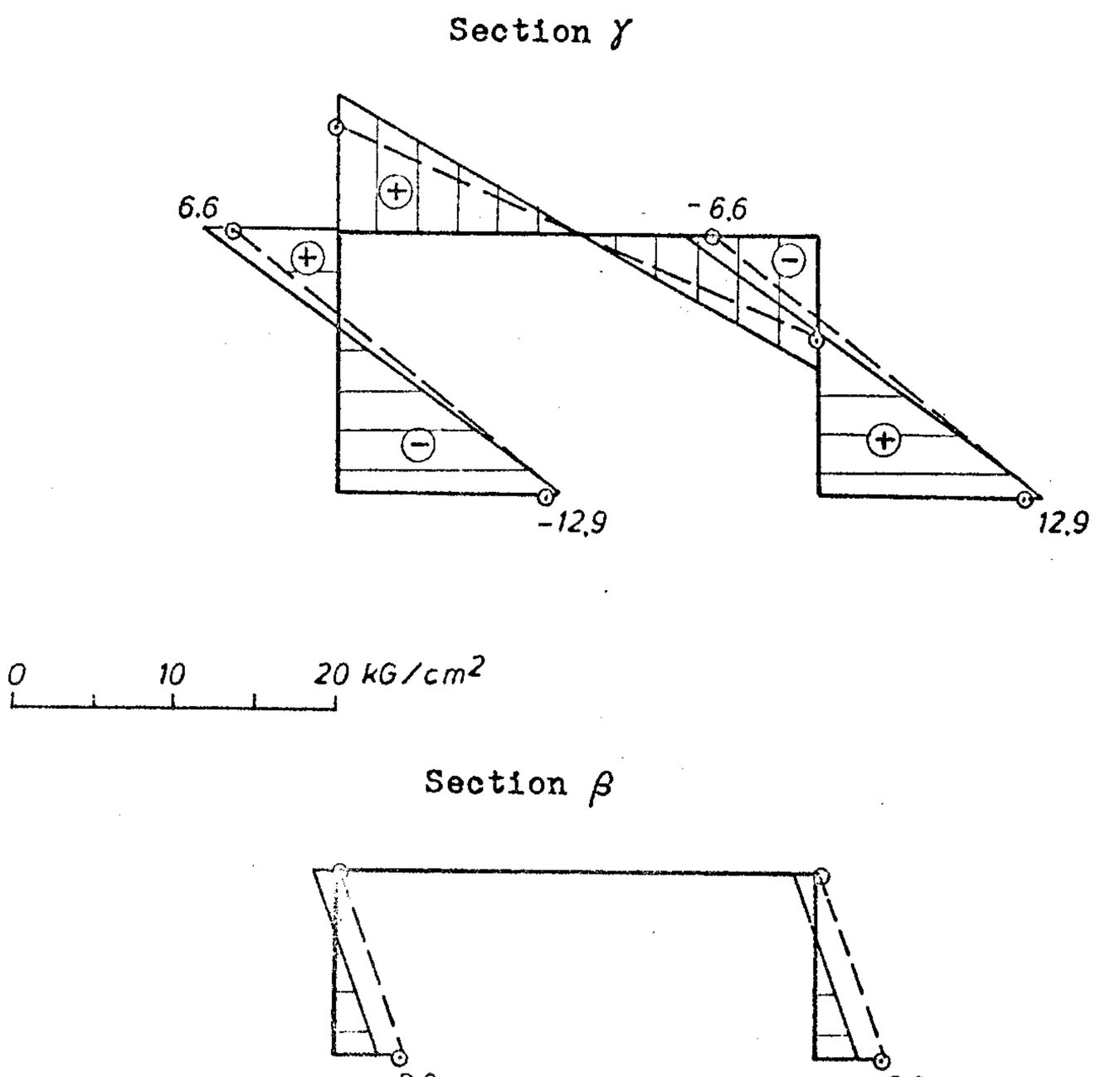

Fig. 11. A comparison of computed warping /normal/ stresses with the experiment and FEM results according to [6]

The warping normal stresses, as calculated with the program are shown in Fig. 11 /full line/ for the case of 5 elements, $\rho = 1$, $\alpha = 1$ The mean of the stress values at the cross section /for the right and left beam element/ is taken as the actual stress magnitude. Computed stresses are compared with the experiment /circles/ and FEM /dashed line/ results and accuracy is found to be sufficient for practical purposes.

4. EXAMPLE B. A BOX-SHAPED CANTILEVER CONSISTING OF OPEN AND CLOSED PRISMATIC PARTS

A simplified hull of an open ship is considered. The hull is idealized as a box-shaped cantilever consisting of open and closed prismatic parts /Fig. 12/ clamped at the stern end of the open hull part. The loading cases to be considered are shown in Fig. 13, the results are, however, presented only for the first, second and seventh load case.

At first the FEM calculations were performed using the NV339 computer program /three-dimensional membrane systems analysis/ from the SESAM system. A finite element mesh assumed is shown in Fig. 14. The mesh consists of 457 joints and 464 rectangular membrane elements. Next the calculations based on the thin-walled beam theory and the transfer matrix method were performed using the computer program described above.

In the first loading condition the cantilever is loaded with point forces that can be reduced to a constant /over the cantilever length/ torsional moment. Special attention was paid to the influence of warping compatability coefficient α on the accuracy of results. The calculations were therefore performed for $\alpha = 1$ and $\alpha = 4.25$ according to /9/, both at the section $z = 120m$ /i.e. at the junction of the open and closed parts/. It should be stressed that $\alpha = 1$ means compatibility of warping coefficient and bimoment, but both the warping and warping /normal/ stresses are discontinuous at this section due to the abrupt change of the cantilever cross section there.

Results of the calculations for the first loading condition are shown in Fig.16 to 27. Results for α determined according to the formula /9/ are marked with full line while those for $\alpha = 1$ are marked with dashed line. Results of FEM calculations are marked with circles.

The conslusion which can be drawn from the above comparison is that a significant improvement in the accuracy can be achieved when the α value according to /9/ is introduced at the junction section of the open and closed parts. However, normal stresses in the closed part differ considerably from the corresponding FEM results, independently of the α value. Likewise the shear stress values at the section $z = 5m$ /close to the clamped end/ and at $z = 125m$ /in the closed part near the junction with the open part/ are inaccurate, independently of the α value.

These inaccuracies are evidently caused by the restrictions of the theory of thin-walled beams itself. It seems that in the case of hull deformations the accuracy might be considerably increased if an appropriate value of α was chosen /the same holds for stresses in the open part/. The calculations were repeated for α determined according to the exact formula worked out by Haslum et al. [3], however, practically the same results as described above were obtained[x]. Further calculations presented in the paper were performed for $\alpha = 4.25$ determined according to the formula /9/.

In the second loading case the cantilever is loaded with a set of longitudinal forces that can be reduced to a horizontal bending moment, constant over the whole beam length, and a bimoment applied at the free end. Particular attention was paid to the coupling between the horizontal bending and torsion according to the condition /10g/. Calculations were performed, with the condition /10g/ taken into account, and repeated with the above mentioned coupling omitted i.e. when the second term in /10g/ is neglected. It should be stressed, however, that in this case pure horizontal bending takes place, as the bimoment applied at the free end may be disregarded /its effect is of a local nature/. Results of calculations for the second load condition are shown in Fig. 28 to 30. The results in the case of pure horizontal bending are marked with full line, while the results for the coupling term taken into account are marked with dashed line. The FEM results are marked with circles, as for the first load condition.

Making allowances for the coupling between horizontal bending and torsion according to the condition /10g/ leads to considerable discrepancies with the results of FEM calculations. Particularly big discrepancies occur in the case of the angles of rotation /they are by one order of magnitude larger than angles determined by FEM/. On the contrary, results obtained in the case of pure horizontal bending /coupling term in /10g/ diregarded/ are close to the FEM results, including also the horizontal displacements. In this case angles of rotation disappear, as the effect of the external bimoment of the value 18840 Tm^2, applied at the free end, may be neglected. The results of FEM callaculatons indicate, however, that a coupling between horizontal bending and torsion actually takes place, because noticeable angles of rotation appear

---

x/ According to the exact Haslum's formula $\alpha = 4.0044$ was obtained instead of $\alpha = 4.25$ as for the first approximation according to /9/.

/Fig. 28/ and normal stress distributions /not presented in this paper/ evidence that a weak bimoment still exists.

In the seventh loading case the cantilever is loaded by distributed forces of constant intensity, applied in the horizontal direction to the bottom. The load simultaneously caused horizontal bending and torsion of the cantilever. Results of calculation are shown in Fig. 31 to 33. Like previously, the results in the case of no coupling between horizontal bending and torsion are marked with full line, the opposite case is shown with dashed line, and the FEM results are marked with circles.

The effect of the coupling term in the condition /10g/ appeared to be far less than in the case of the constant /over the beam lenght/ horizontal bending moment. It can easily be explained as for a uniformly distributed load the horizontal bending moment at the junction of the open and closed parts, which appear in /10g/, is far less than in the previous case. Nevertheless the significant improvement in accuracy of calculations of angles of rotation can be achieved, too, if the coupling is disregarded.

Eventually a modification of the expression /10g/ has been introduced, to improve calculation results. Instead of /10g/ the following expression has been programmed

$$M^{R}_{\Omega,n} = \frac{1}{\alpha_n}\left[M^{L}_{\Omega,n} - M^{L}_{x,n}\left(e_{n+1} - e_n\right)\right] - \bar{M}_{\Omega,n} \qquad /16/$$

i.e. the second term in /10g/ is considered to be the bimoment applied at the left side of section n. The appropriate calculation results are drawn up using dot-and-dash line in Figs. 28 to 33.

In general a great improvement can be observed in comparison with the original approach /dashed line/. The results are also better /or equivalent/ than those obtained after neglecting the second term in /10g/ i.e. when coupling effect is disregarded. The modification also improves accuracy of results of normal stress calculations /not presented in the paper/ as compared with pure bending /excluding the sections very close to the junction between open and closed parts/.

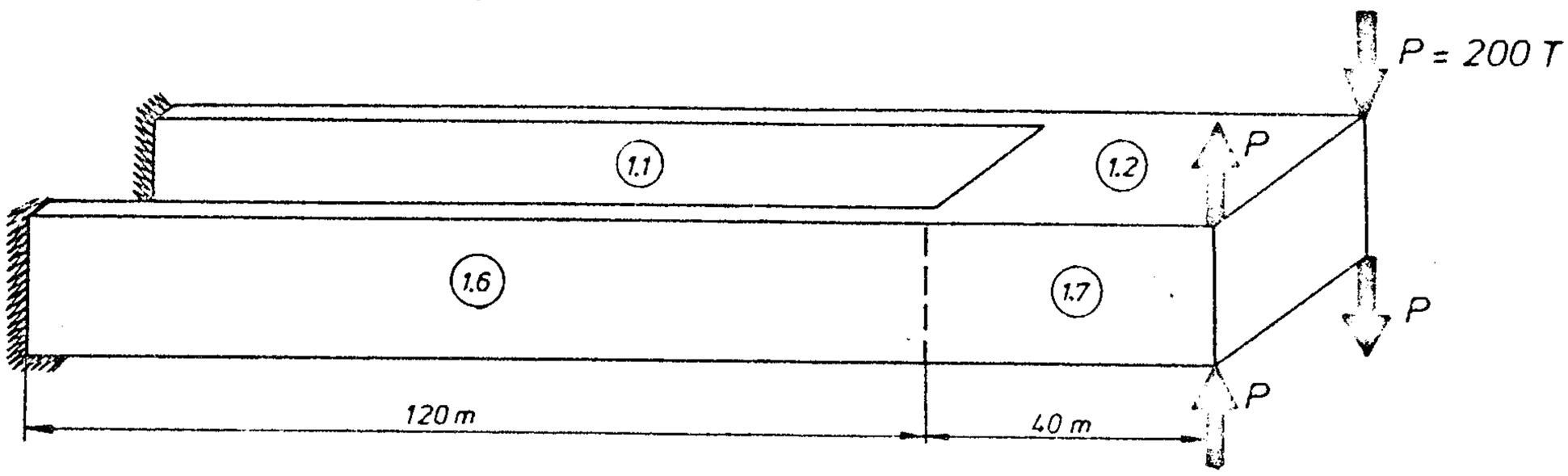

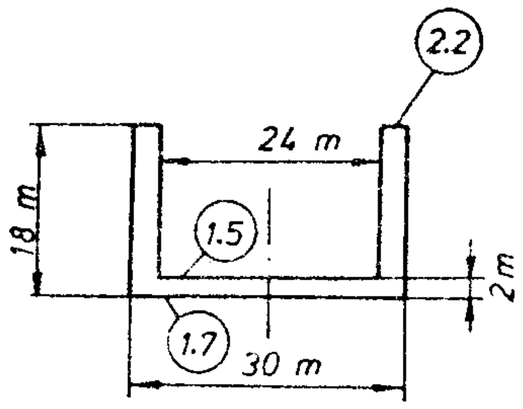

I_ω = 11278 m^6
I_T = 11.096 m^4
y_c = -6.0837 m
ϱ = 1.05

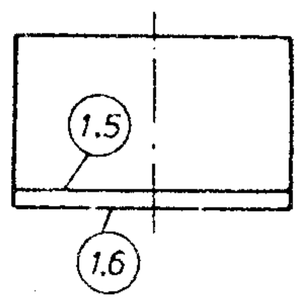

I_ω = 624.4 m^6
I_T = 190.95 m^4
y_c = 5.184 m
ϱ = 4.344

Fig. 12. A box-shaped cantilever with open and closed partes /wall thickness given in cm/

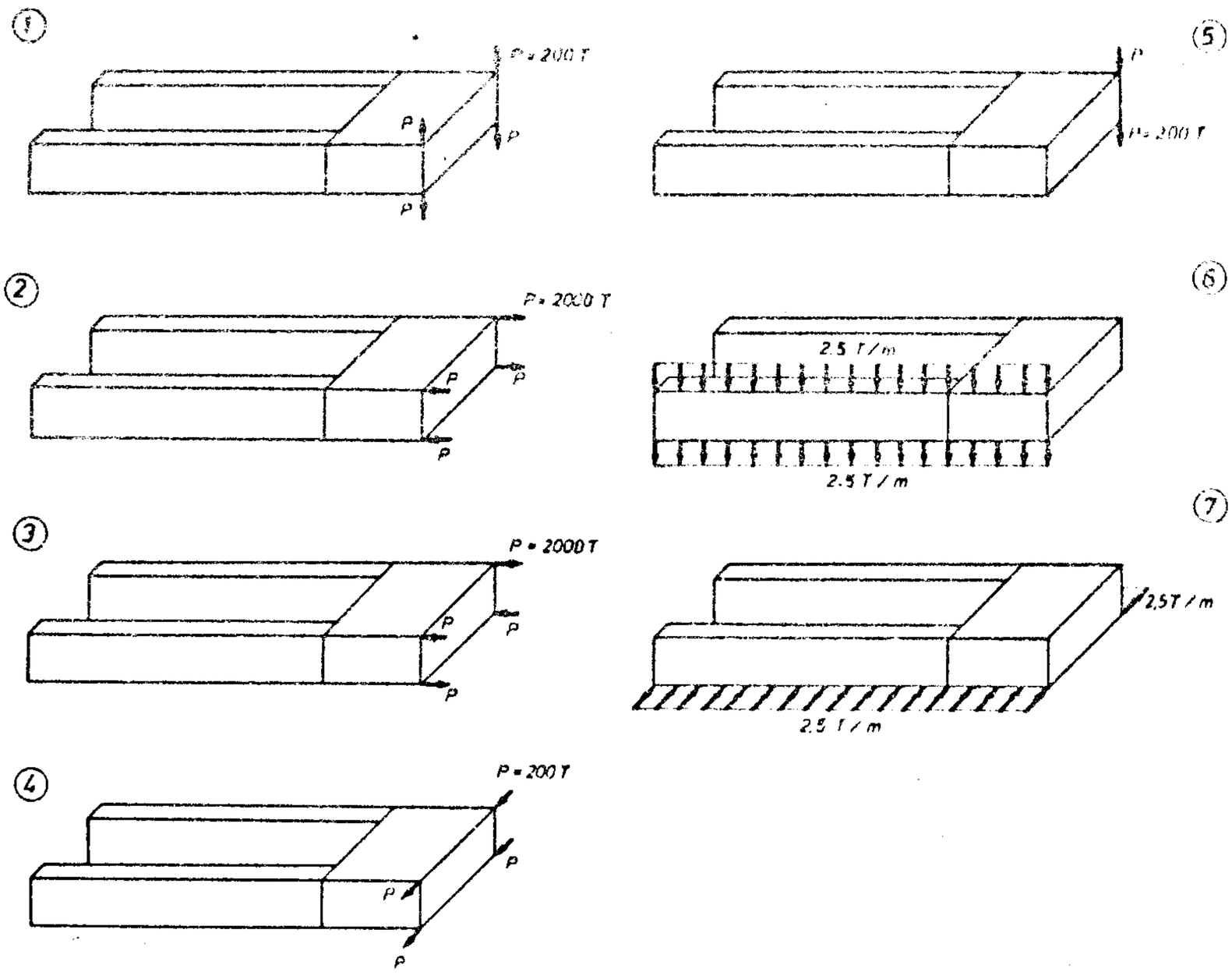

Fig. 13. Loading cases assumed in calculations

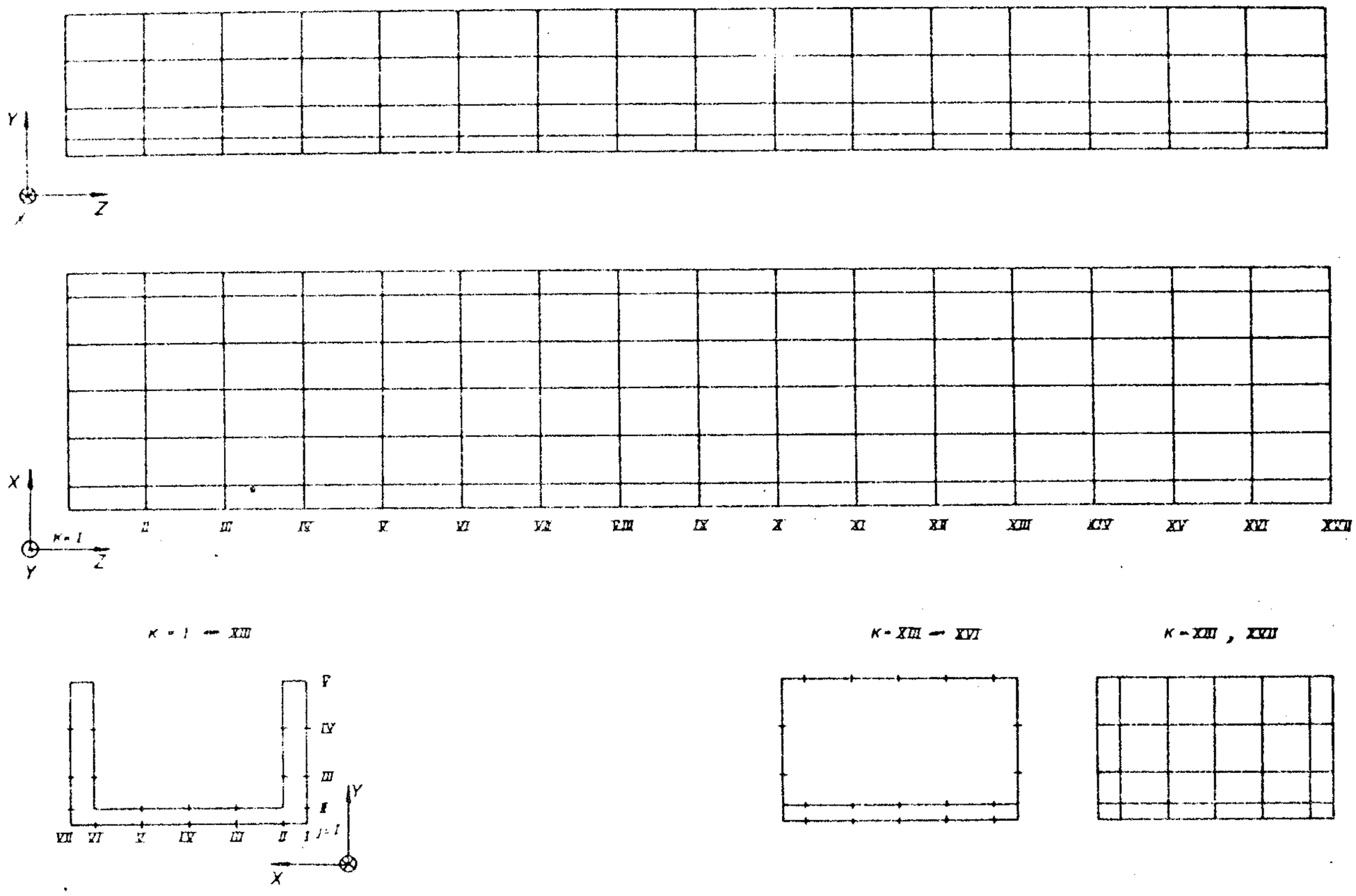

Fig. 14. A finite element mesh assumed in calculation using NV339

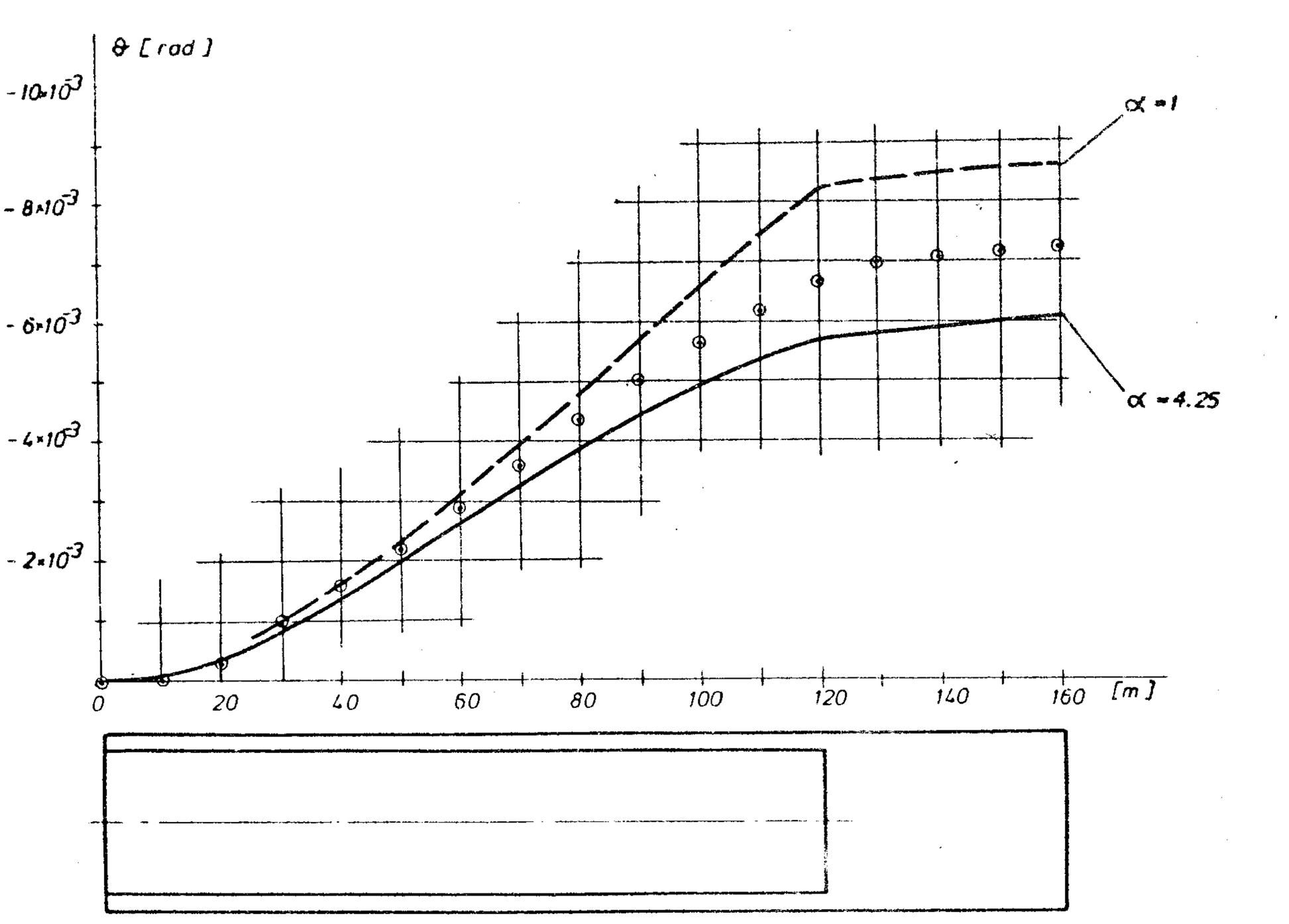

Fig. 15. Angles of rotation for the first loading case

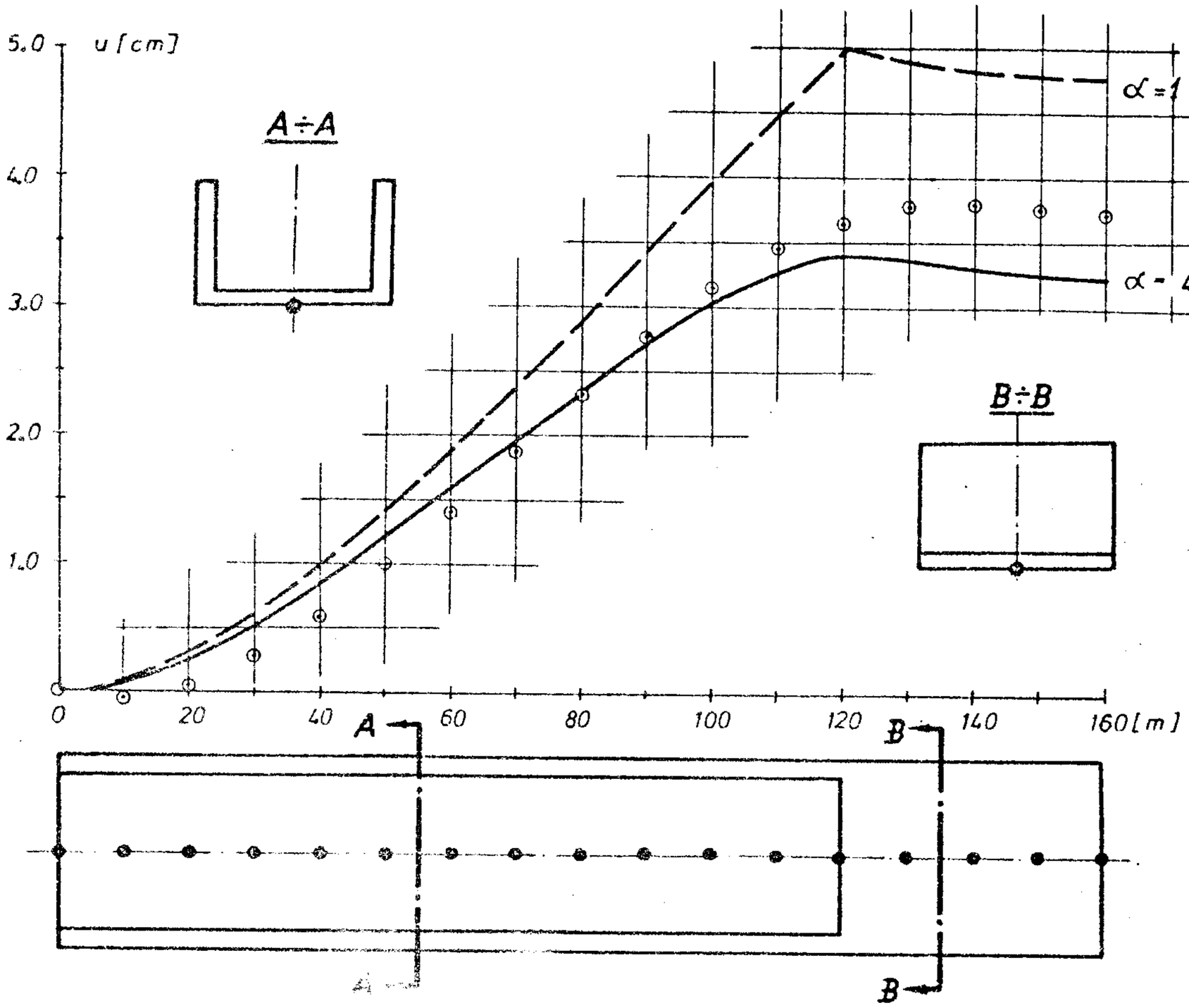

Fig. 16. Horizon[illegible] displacements for the first loading case

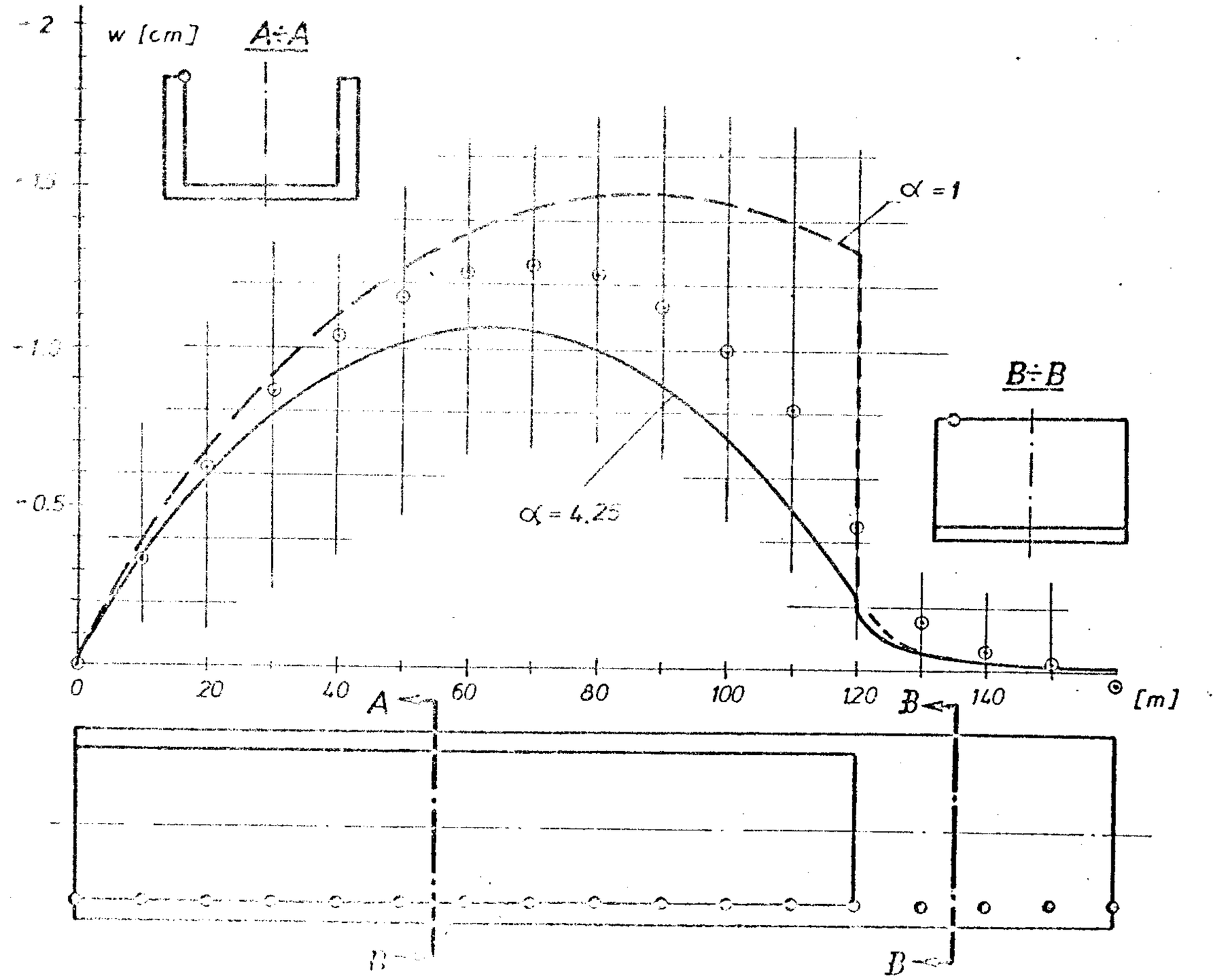

Fig. 17. Warping for the first loading case

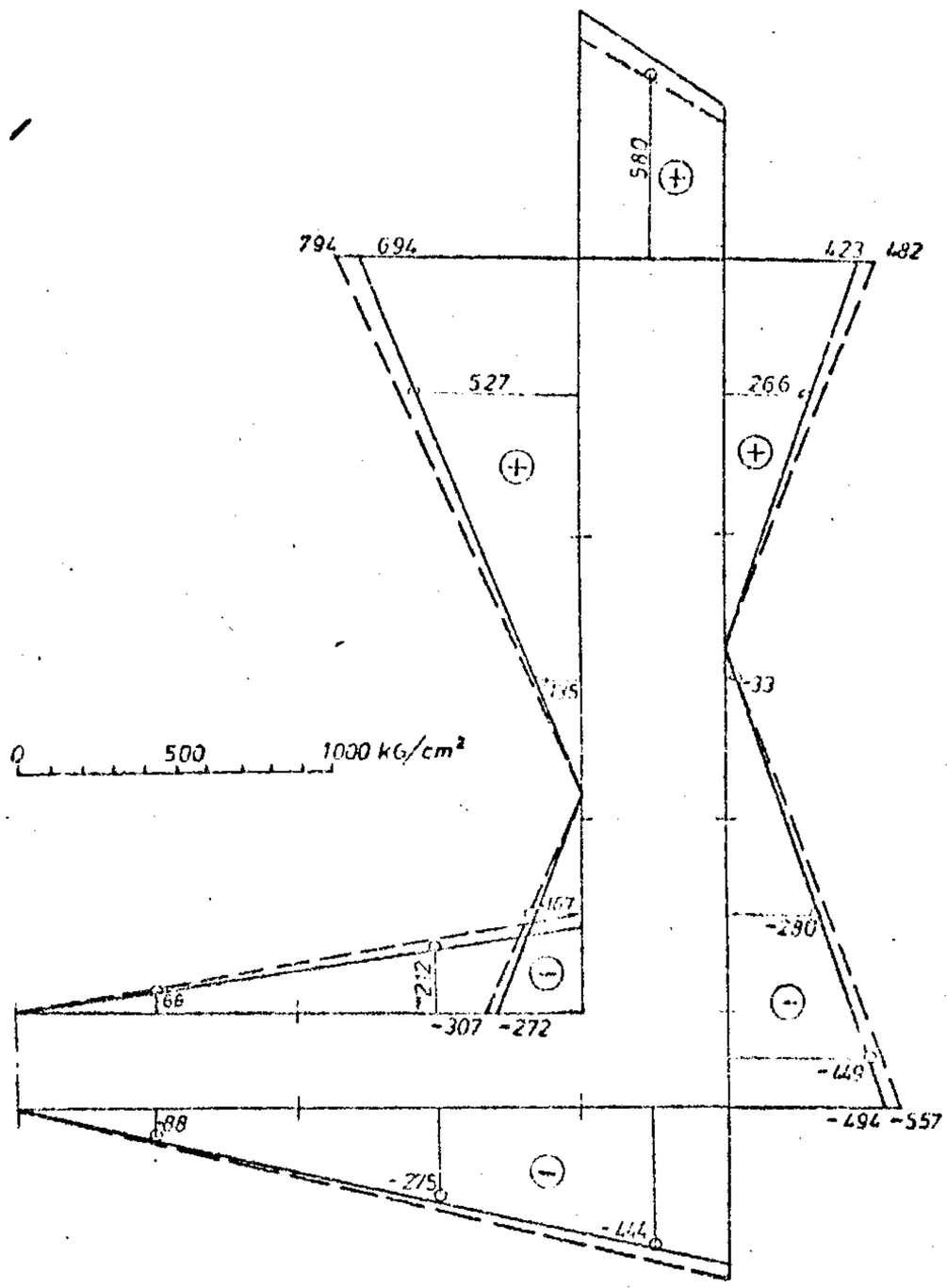

Fig. 18. Normal stresses at section z = 5 m for the first loading case

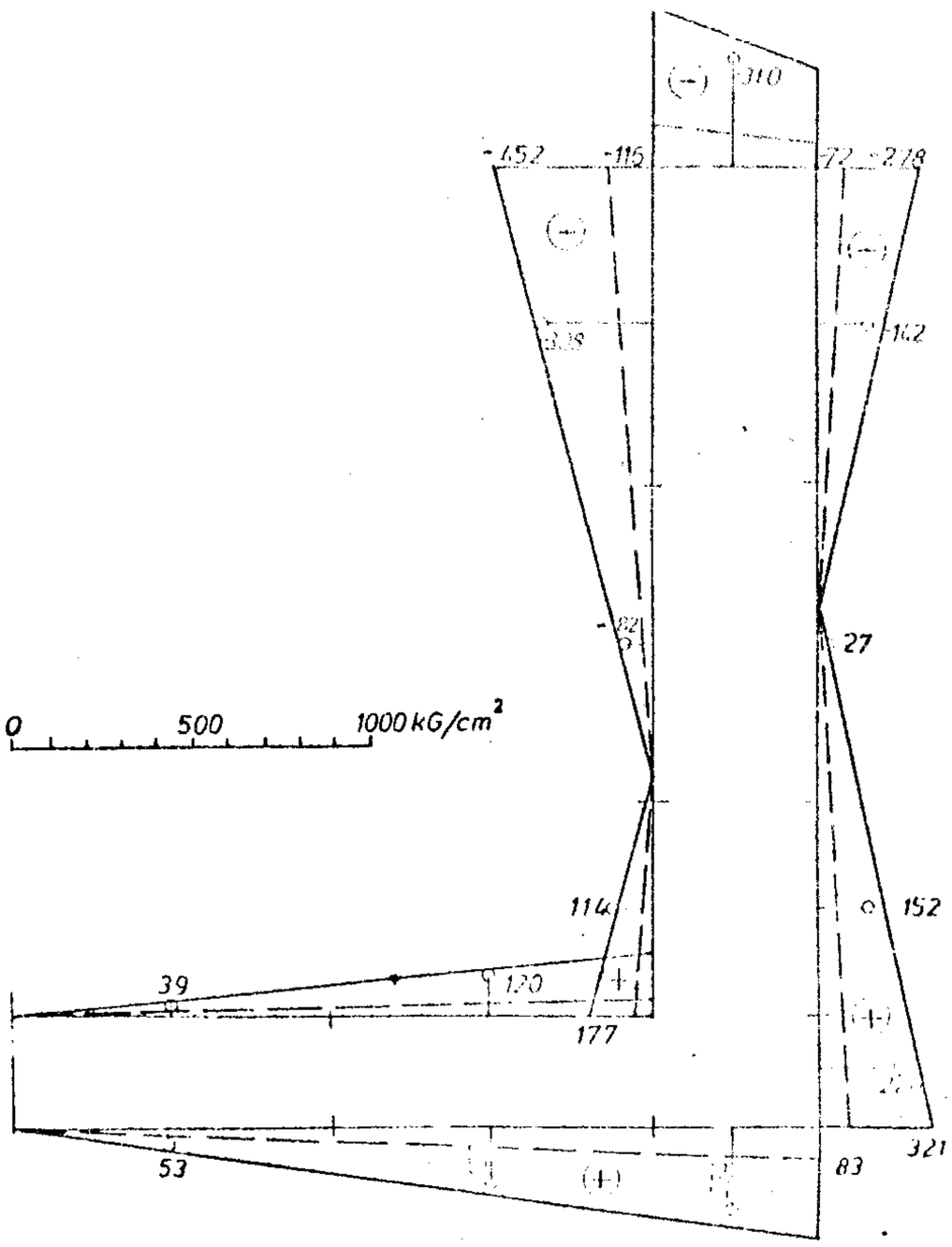

Fig. 19. Normal stresses at section z = 105 m for the first loading case

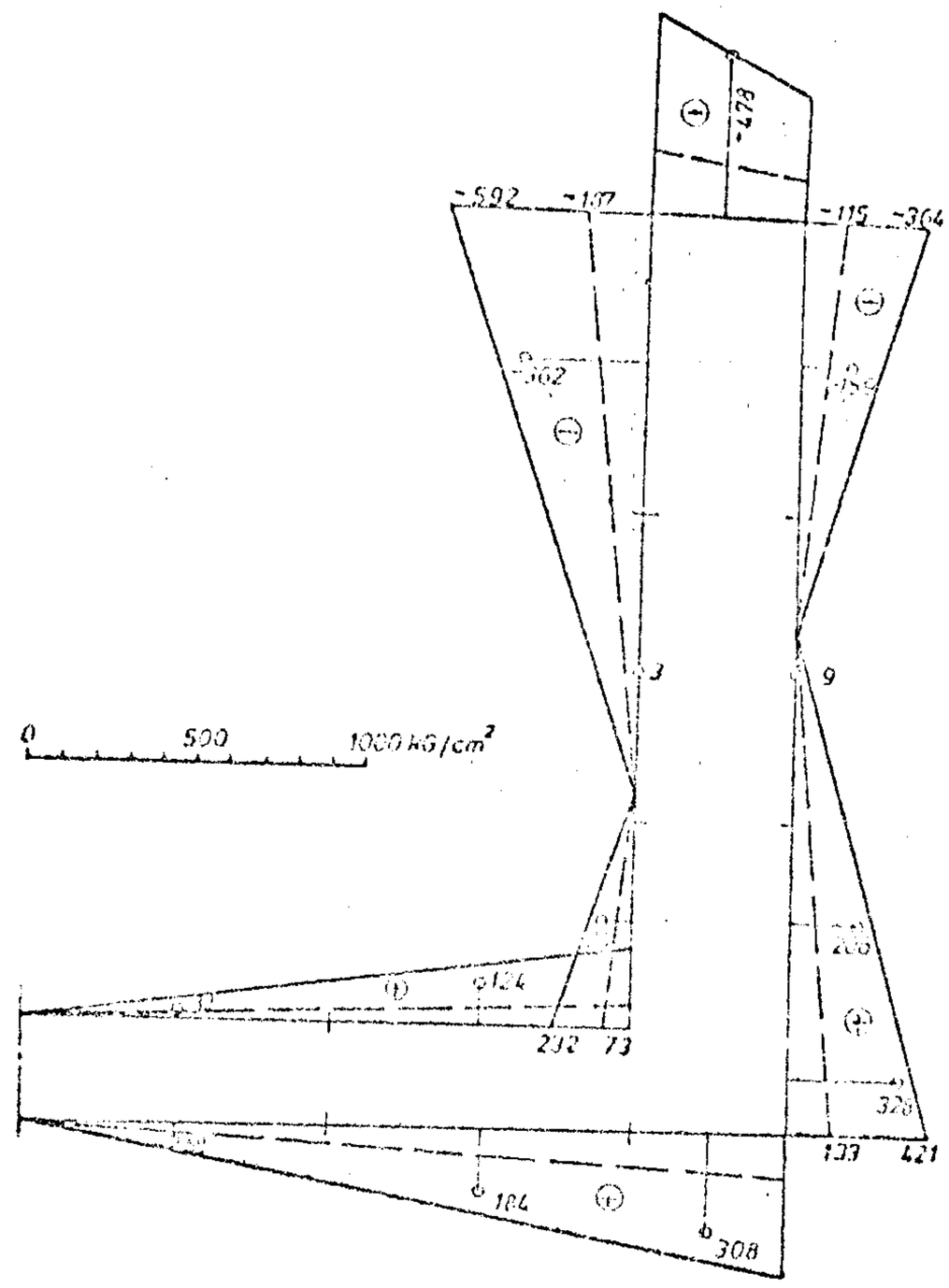

Fig. 20. Normal stresses at section z = 115 m for the first loading case

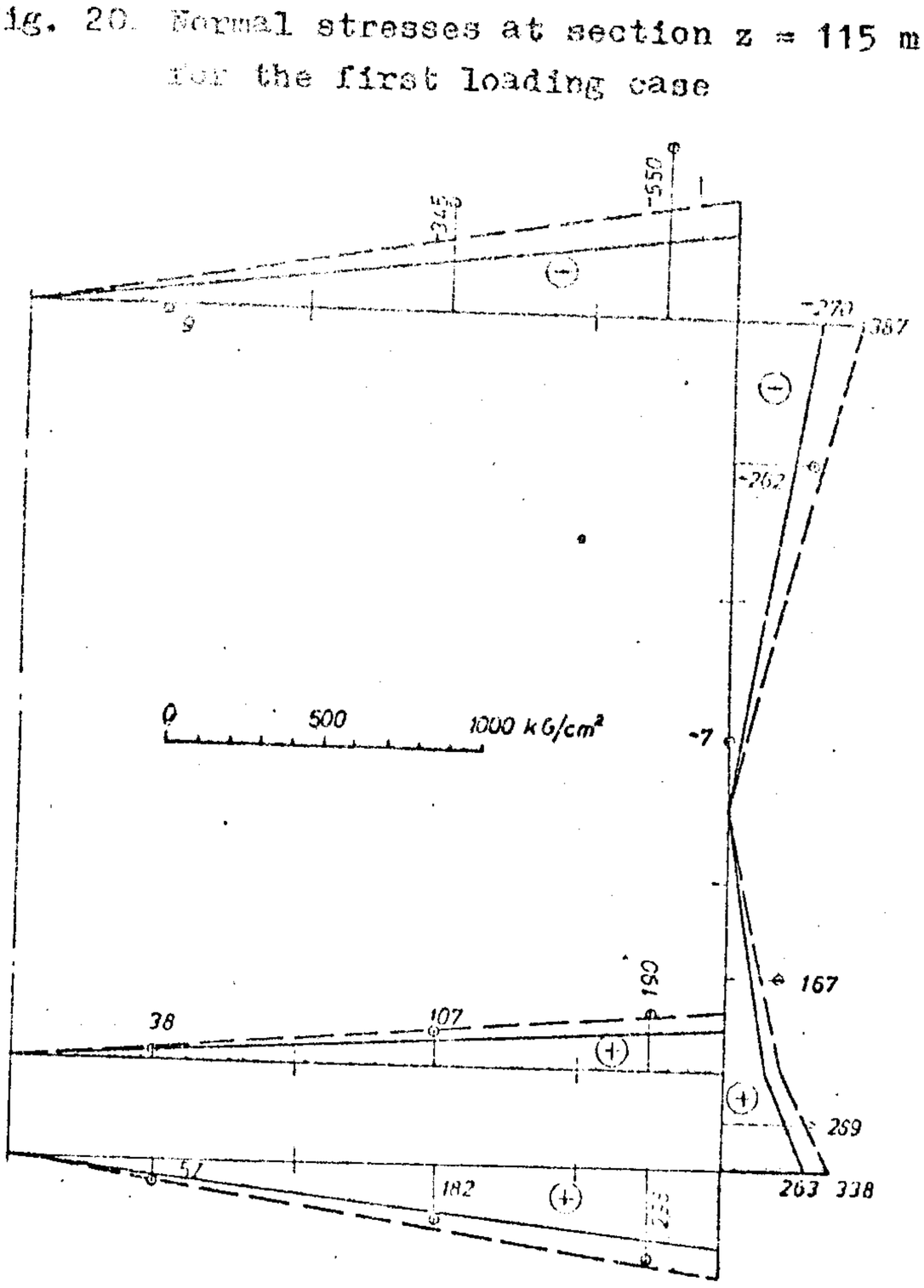

Fig. 21. Normal stresses at section z = 125 m for the first loading case

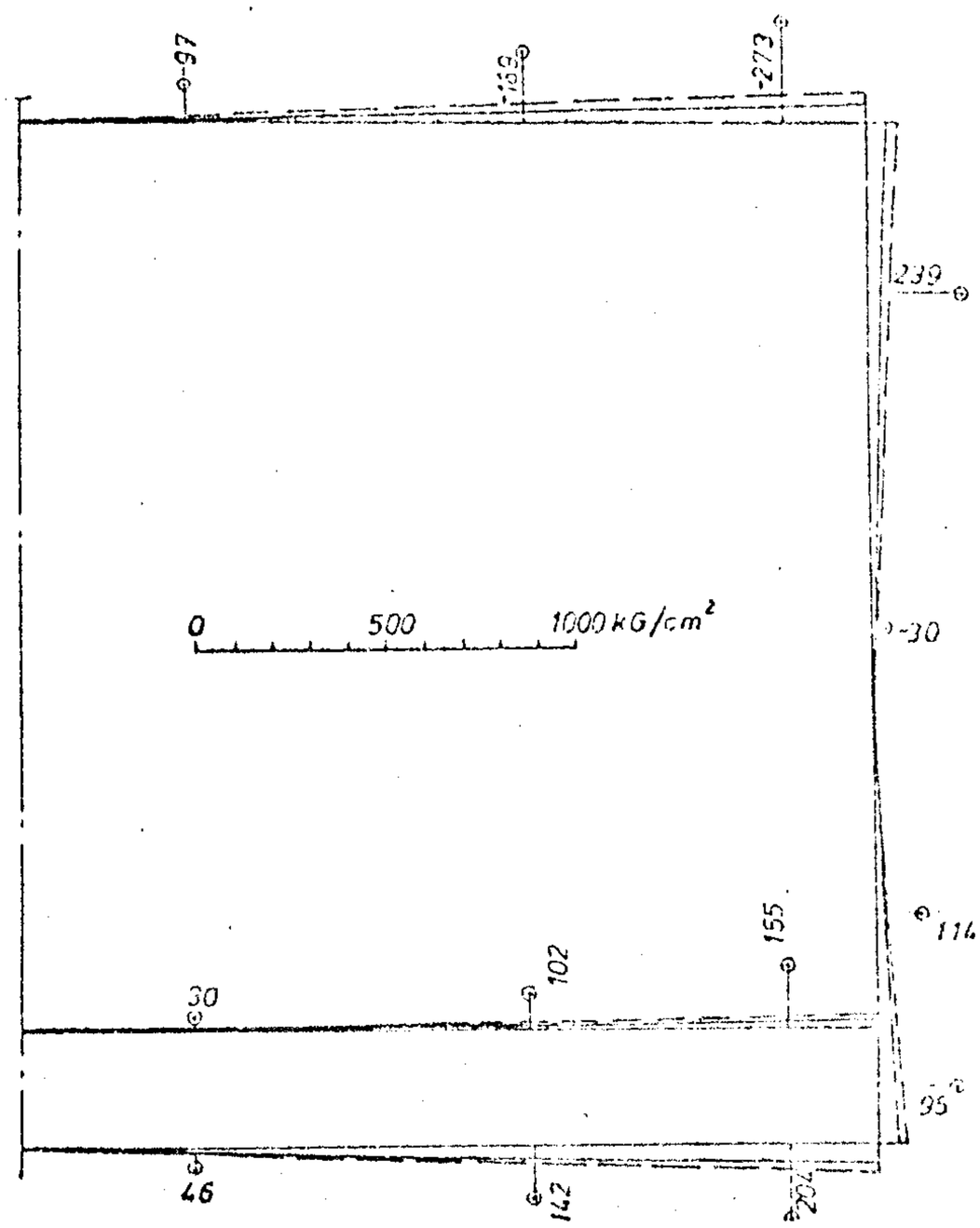

Fig. 22. Normal stresses at section z = 135 m
for the first loading case

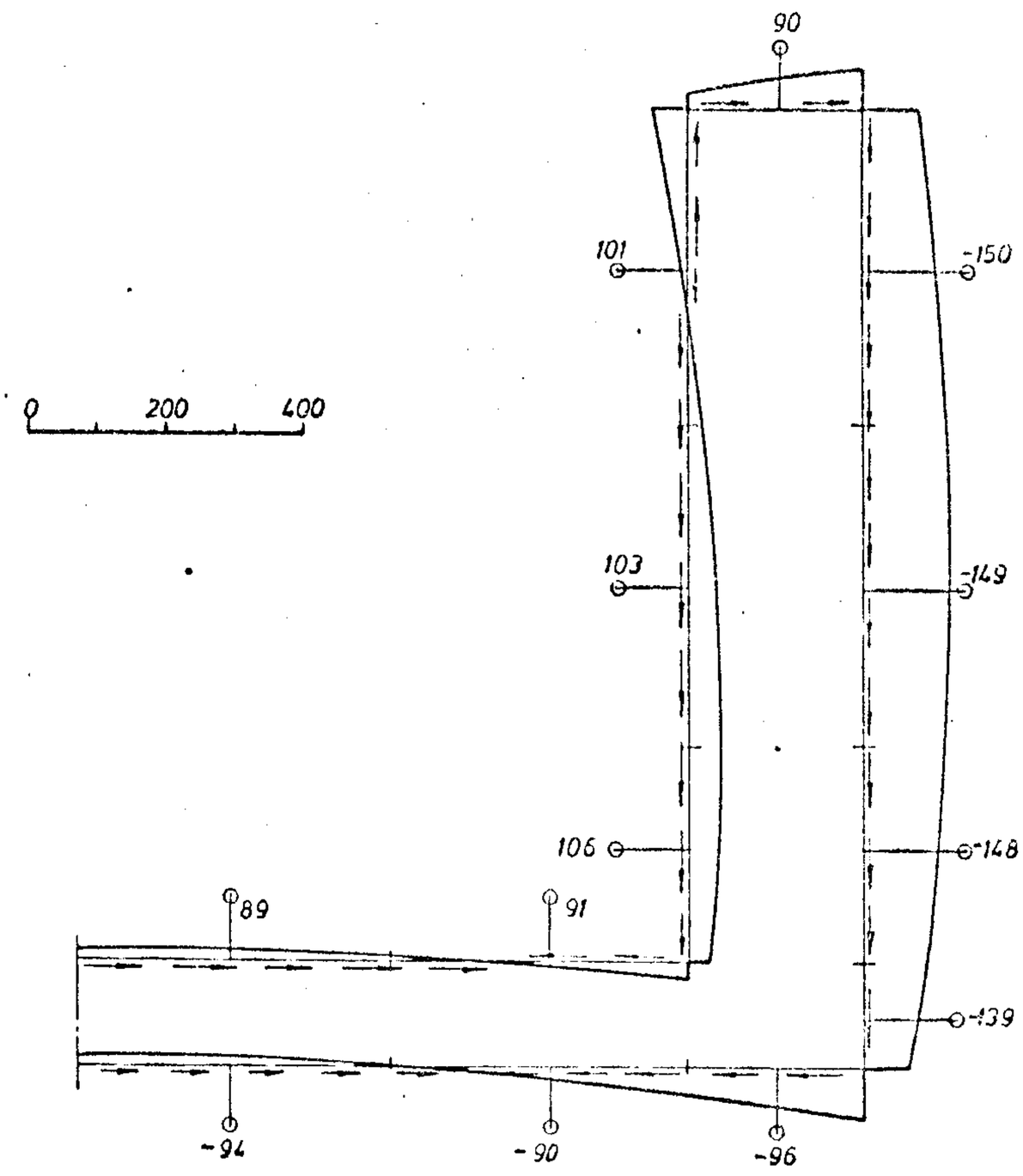

Fig. 23. Shear stresses at section z = 5 m
for the first loading case

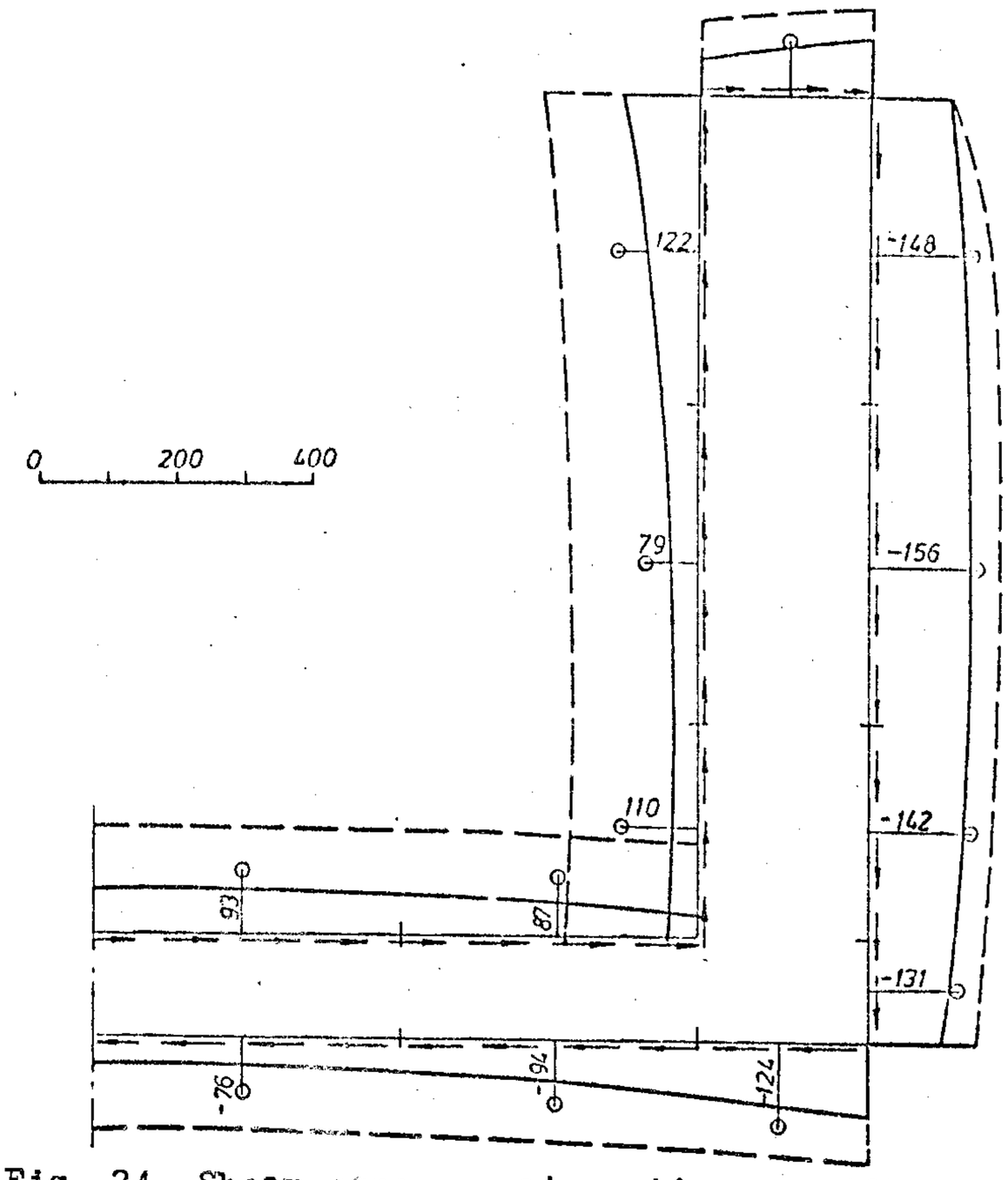

Fig. 24. Shear stresses at section z = 105 m for the first loading case

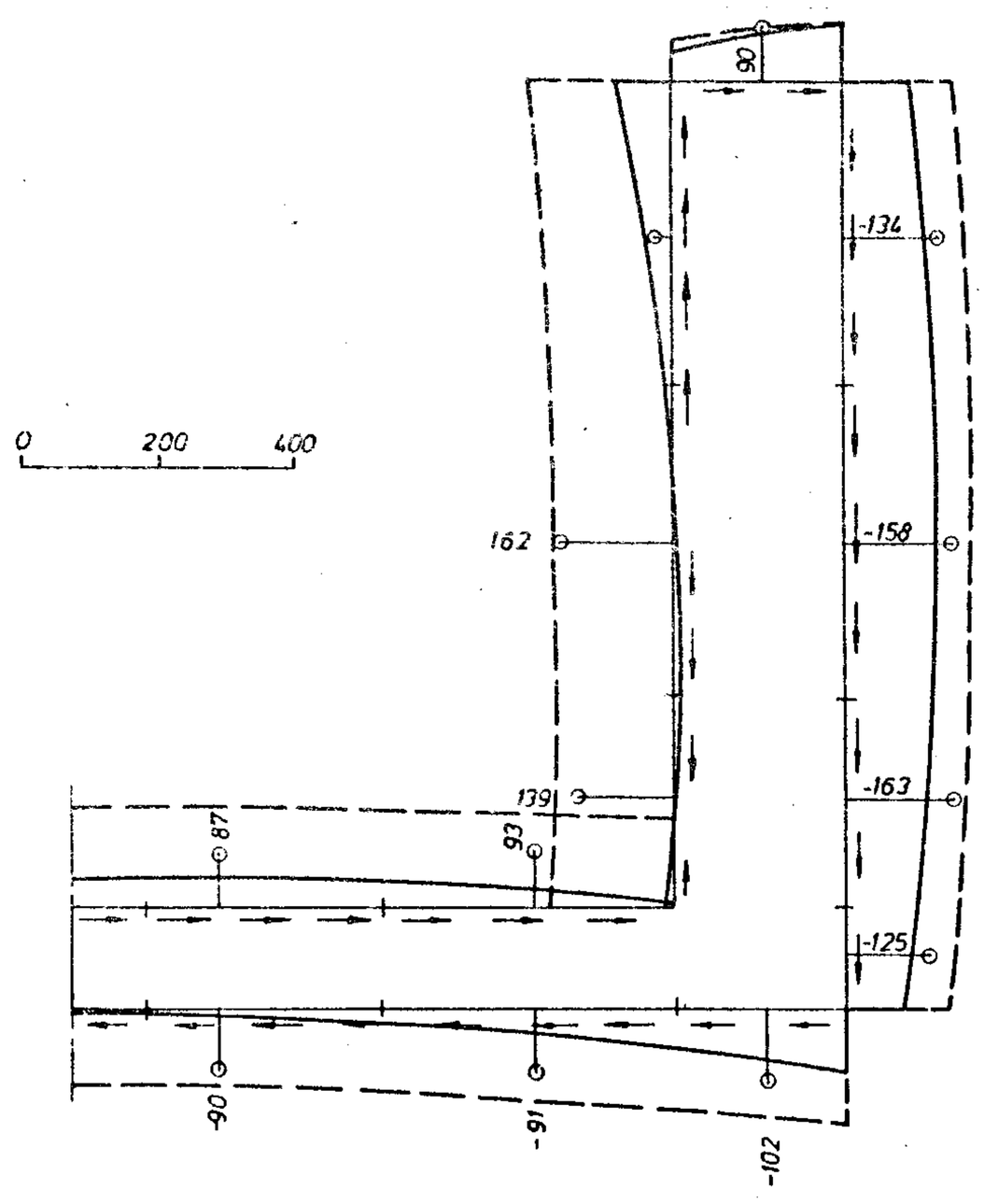

Fig. 25. Shear stresses at section z = 115 m for the first loading case

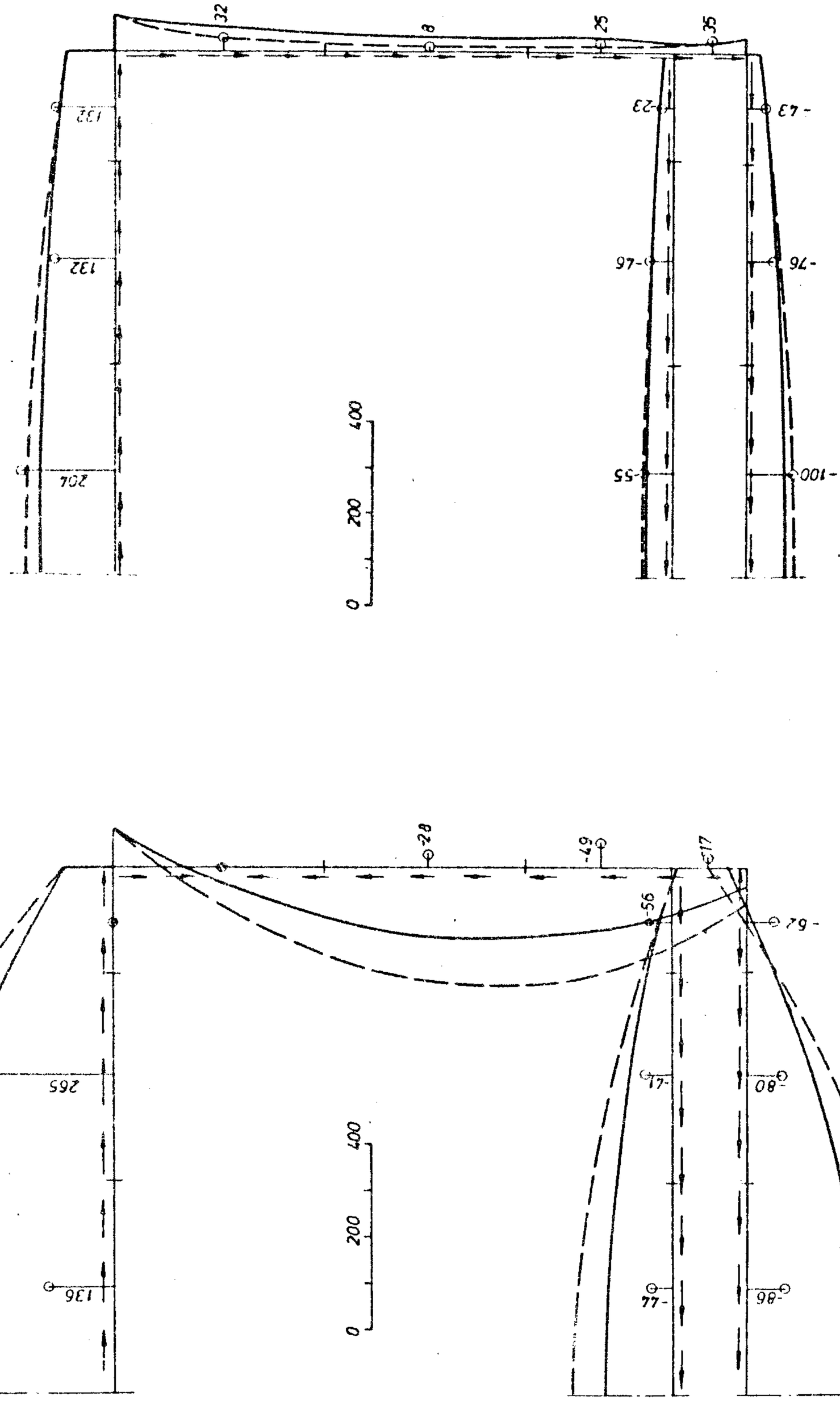

Fig. 27. Shear stresses at section z = 135 m
for the first loading case

Fig. 26. Shear stresses at section z = 125 m
for the first loading case

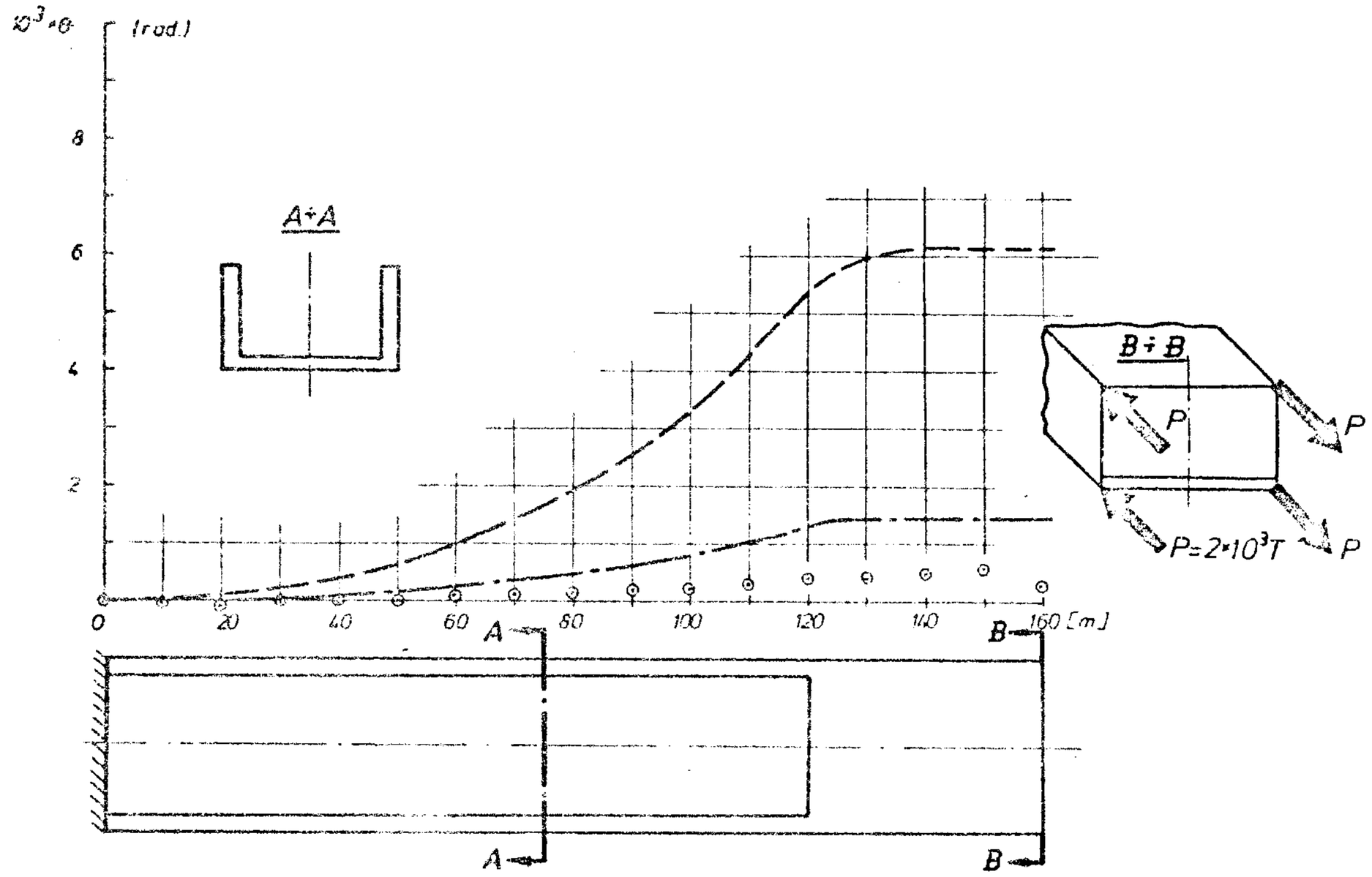

Fig. 28. Angles of rotation for the second loading case

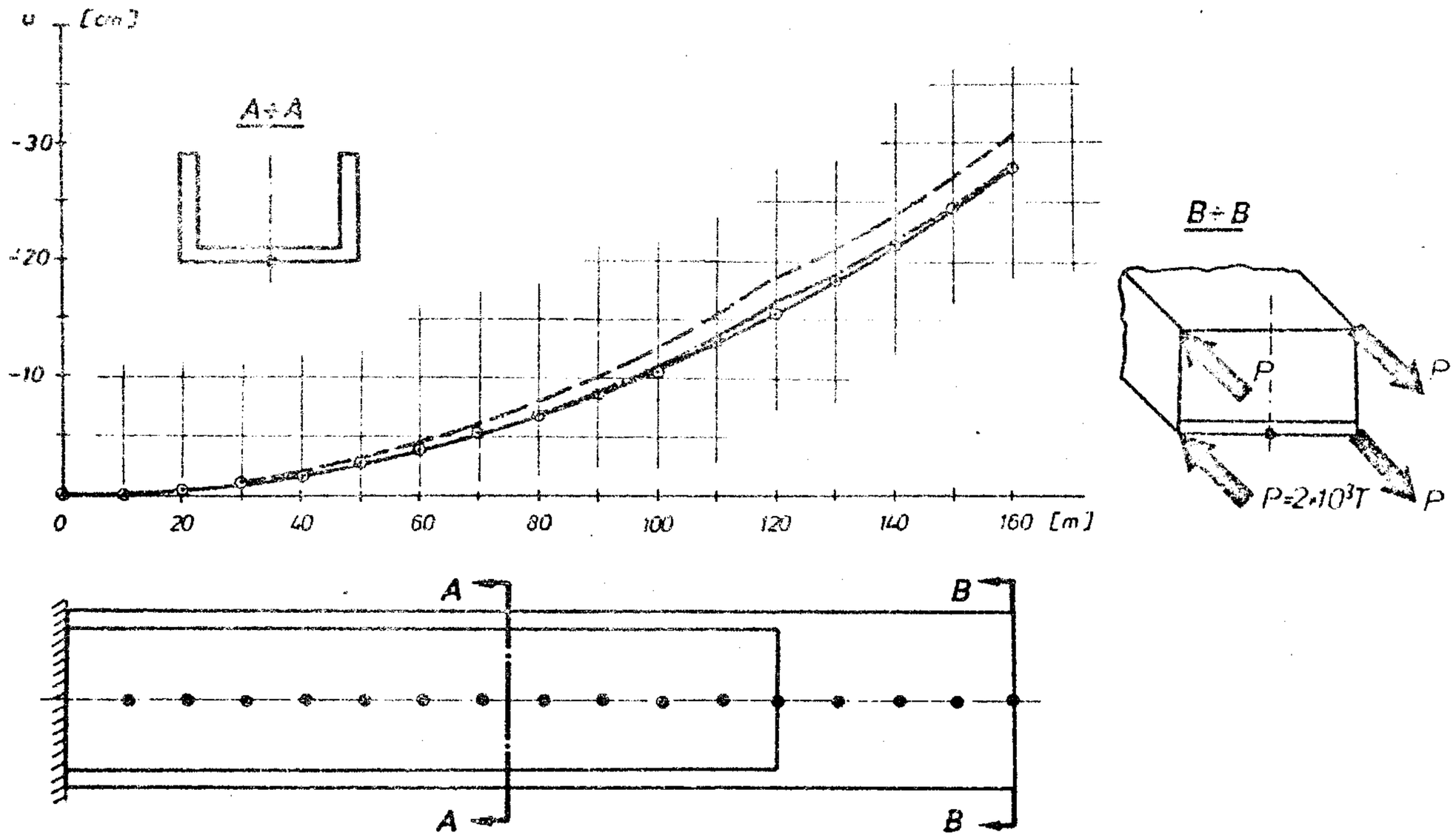

Fig. 29. Horizontal displacements for the second loading case

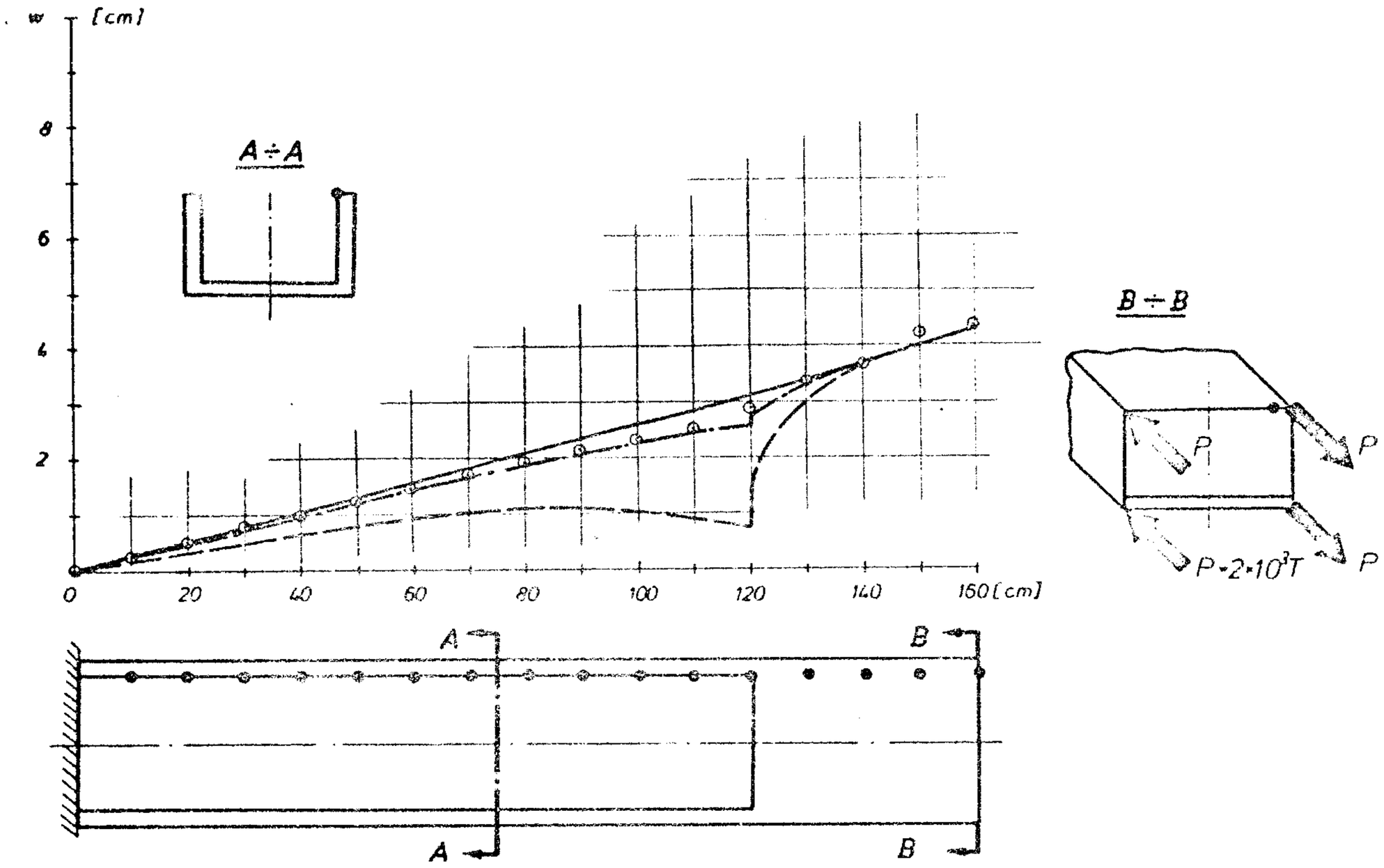

Fig. 30. Longitudinal displacements for the second loading case

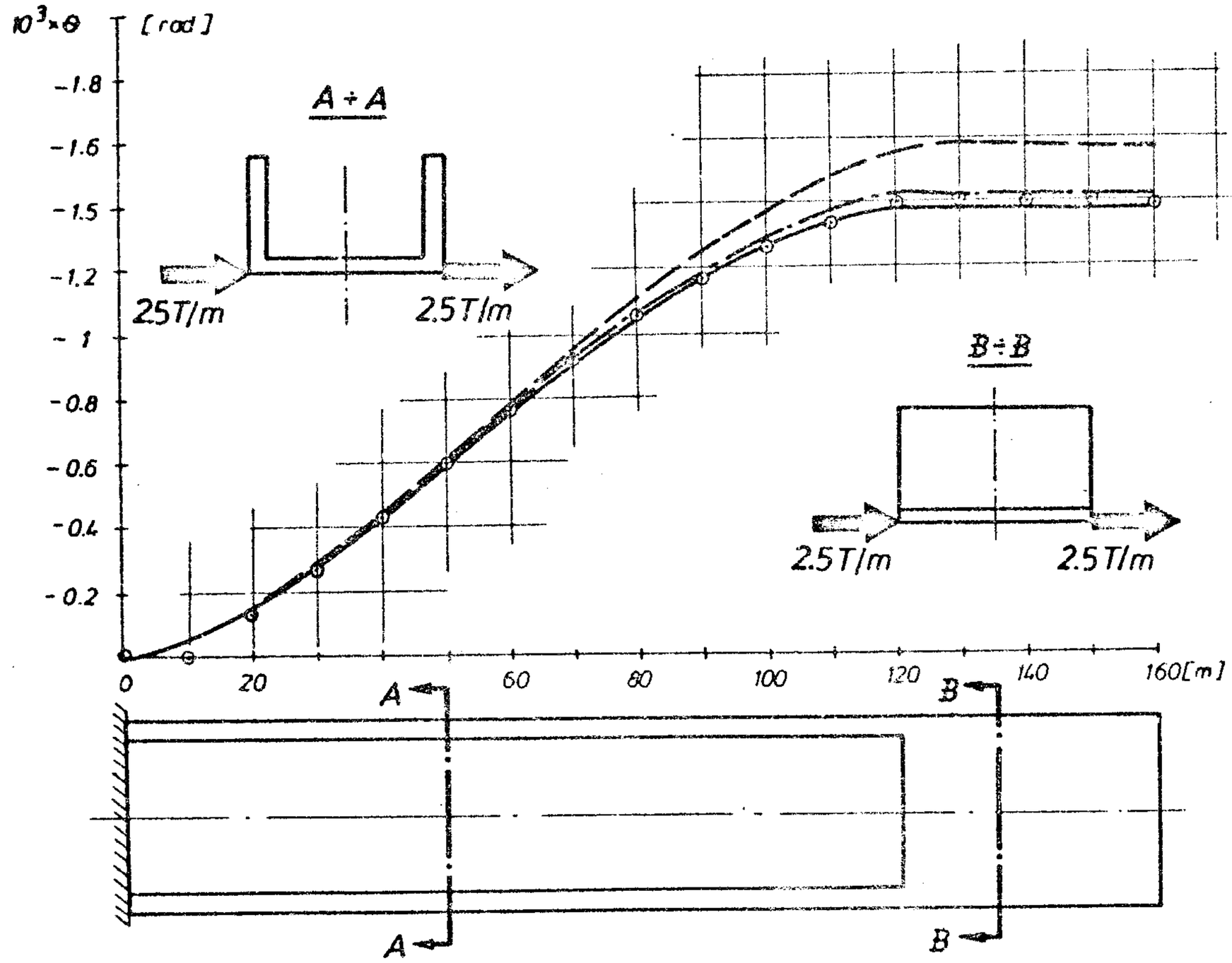

Fig. 31. Angles of rotation for the seventh loading case

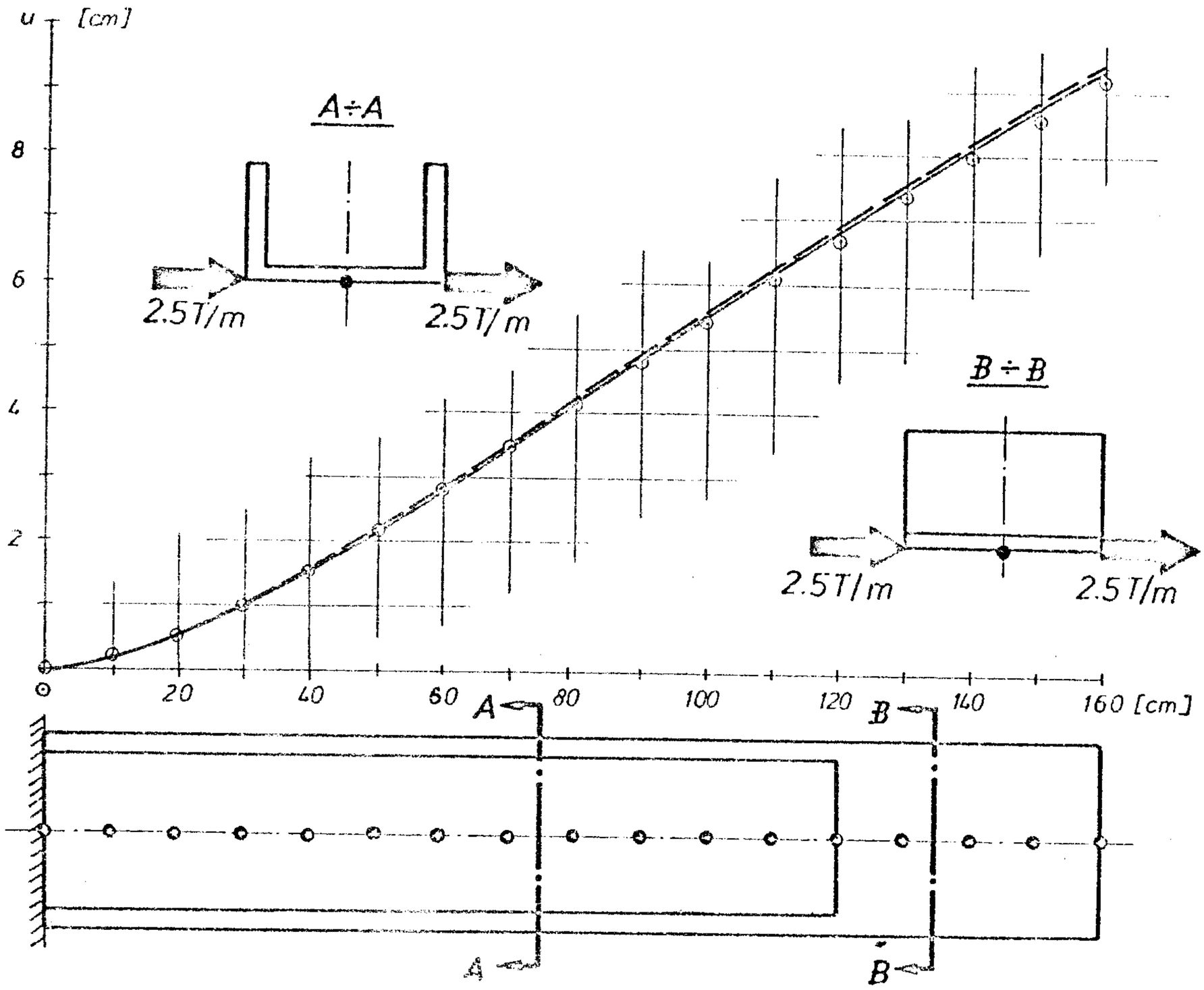

Fig. 32. Horizontal displacements for the seventh loading case

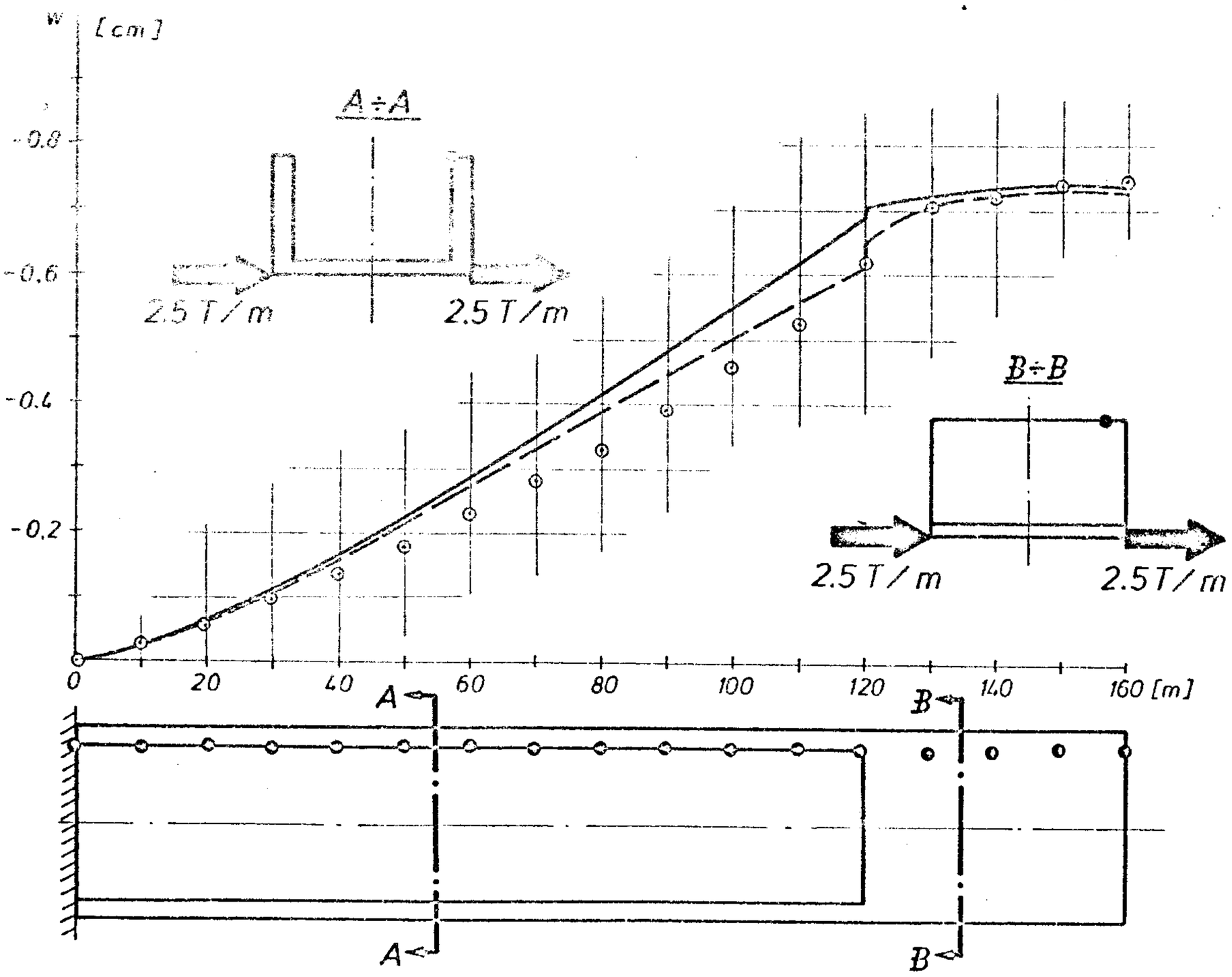

Fig. 33. Longitudinal displacements for the seventh loading case

5. EXAMPLE C. CROSS SECTION PROPERTIES OF A 116 000 DWT OBO CARRIER

An idealization of the midship section of a 116.000 DWT OBO Carrier is shown in Fig. 34. The hull shell is idealized as a composition of rectilinear elements which are defined by nodes and thicknesses. Longitudinals are treated as areas concentrated in nodes.

All closed areas /cells/ are to be opened through cutting in such a way that no element is disconnected with the rest of the structure. The cuts create some new free ends and appropriate new nodes are to be introduced there. They are called "common nodes" as their coordinates are the same as the coordinates of other nodes belonging to the nearest elements.

After the cuts have been introduced, sense is to be given to all rectlinear elements of the equivalent open cross section in such a way that a tree structure is created, with the start point at an arbitrary node on the axis of symmetry of the cross section /node number 1/. The start node of any element has smaller number than the end node. The number of the last node is higher by 1 than the total number of rectilinear elements.

Part A of program enables to obtain the following cross section properties:

- cross section area A_p ;
- shear area in x direction A_x ;
- shear area in y direction A_y ;
- moment of intertia about y axis J_{xx} ;
- moment of inertia about x axis J_{yy} ;
- ordinate of the centre of gravity e_y ;
- ordinate of the shear centre y_c ;
- sectorial moment of inertia J_ω ;
- St. Venant torsional moment of inertia I_T ;
- coefficient ρ ;

Moreover, the program prints out unit longitudinal displacements due to bending and torsion, as well as unit shear flows due to shear and torsion.

The cross section properties of a 116 000 OBO Carrier are given in Fig. 35 /in the framed part/. Among them the shear areas A_x and A_y are of a special significance.

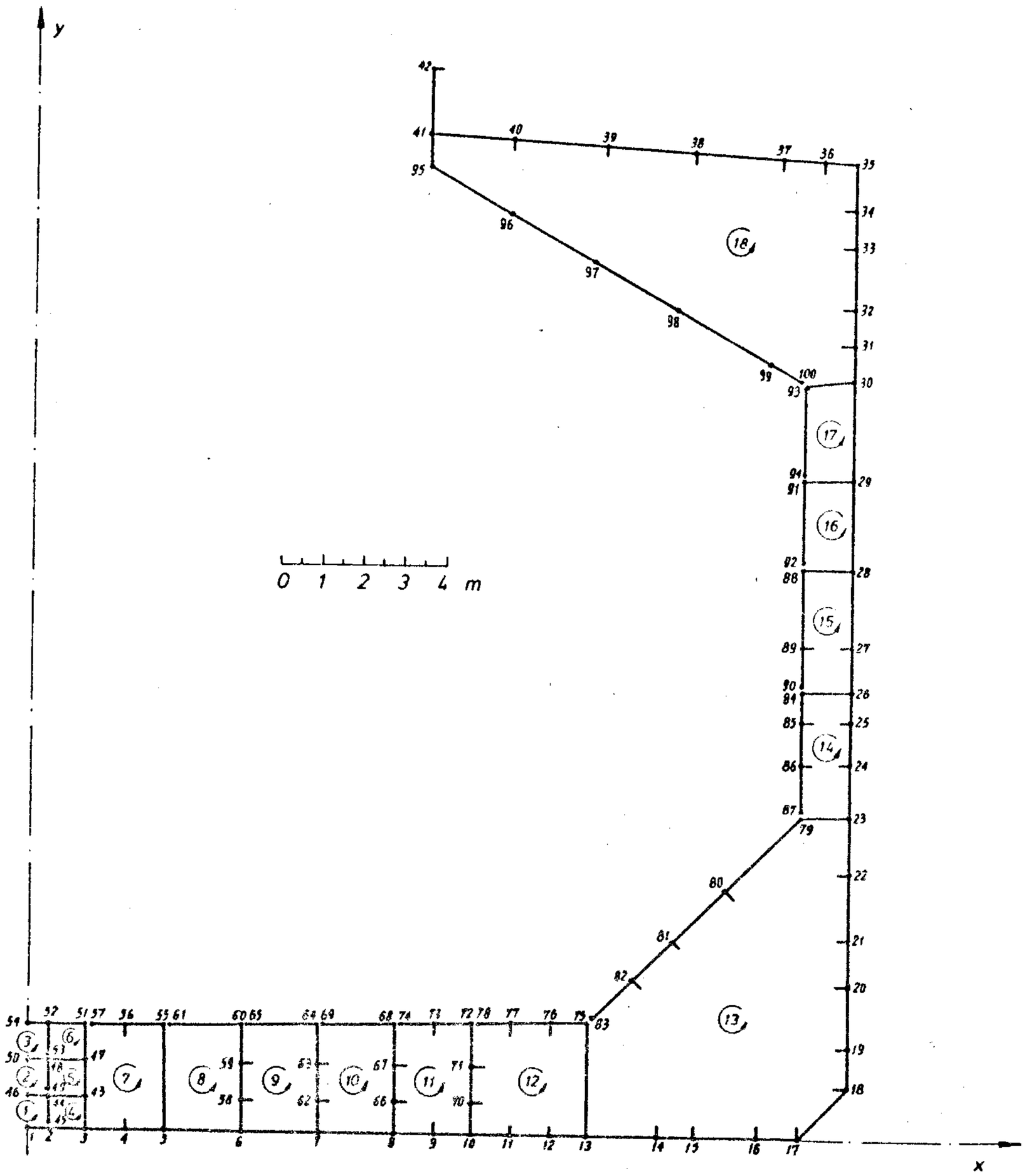

Fig. 34. An idealization of the midship section of a 116 000 DWT OBO Carrier

They are determined according to the exact formulae

$$A_x = \frac{J_{xx}^2}{\int_F \frac{\tilde{S}_x^2}{t^2}\,dF} \quad ; \qquad A_y = \frac{J_{yy}^2}{\int_F \frac{\tilde{S}^2}{t^2}\,dF}$$

These make it possible to determine more precisely not only the hull deformations, but also ship's natural frequencies /in particular those of the higher orders/.

Using part C of the program it is possible to obtain longitudinal displacements as well as shear and normal stresses /due to hull bending, shear and torsion/,

either for the hull response parameters given in the data, or directly, when the parts A, B and C are executed in a single computer run. Basides, total longitudinal displacements as well as total shear and normal stresses are printed out.

Shear stresses τ_y due to the vertical shear force are shown in Fig. 35 for the case under consideration. Discontinuities caused by longitudinals as well as the changes of shell thickness can be noticed on the τ_y diagram.

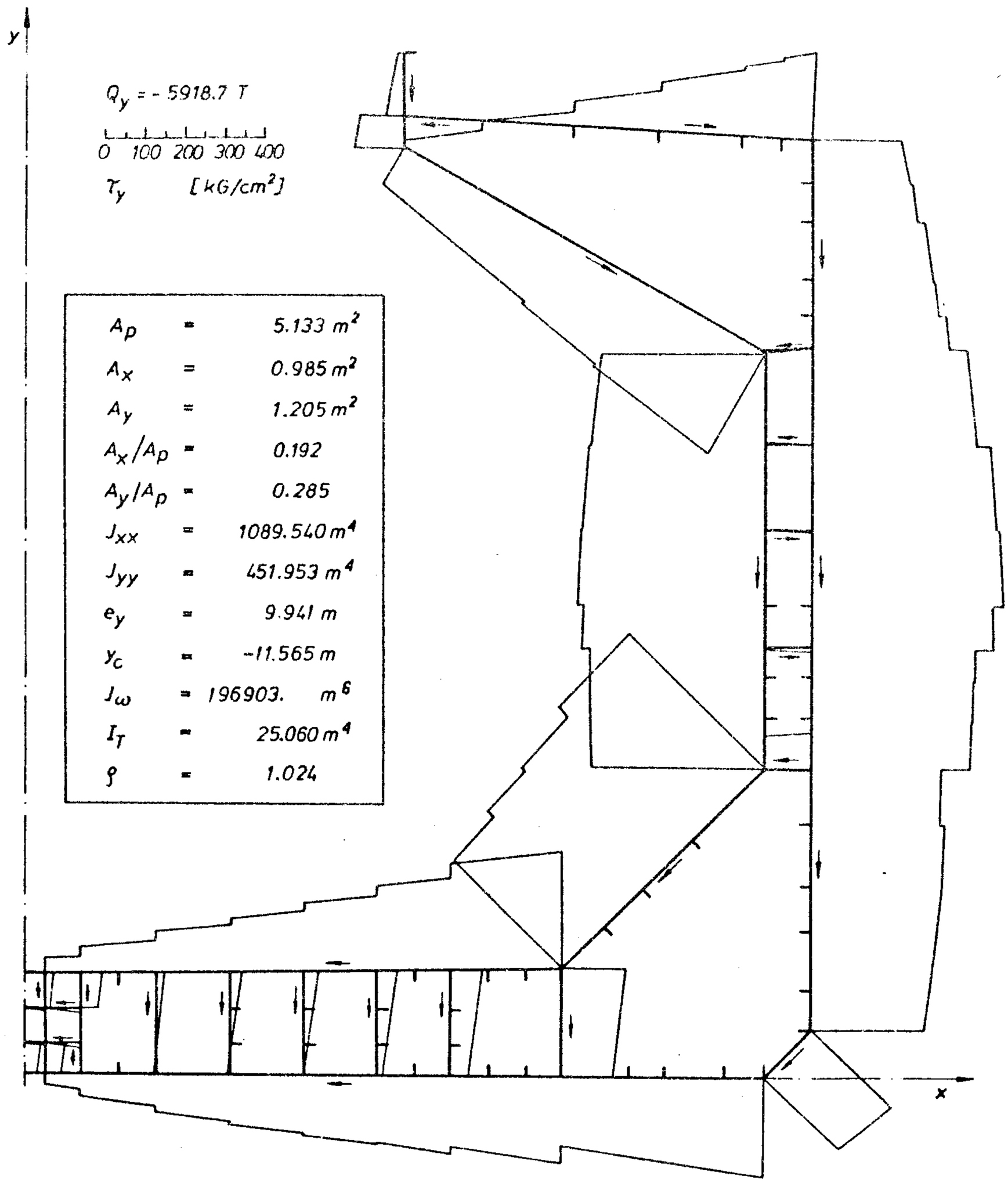

Fig. 35. Cross section properties and shear stresses τ_y diagram

6. EXAMPLE D. TORSION ANALYSIS OF A 163.4 m LONG SEMICONTAINER SHIP

A semicontainer ship is considered with the engine room at stern and the following general data:

length between perpendiculars	L	=	163,4 m
breadth moulded	B	=	25,3 m
height /to the upper deck/	H	=	13,4 m
draught	T	=	9,95 m
block coefficient	δ	=	0.677
waterplane coefficient	α	=	0.833

The ship has a double hull structure at its middle part, as well as a double longitudinal bulkhead at its diametral plane. There are two rows of large hatches in the upper deck and a large single hatch in the foredeck. Deck stringers are narrow in comparision with the transverse deck strips which are broad and stiff, as it is usually done in semicontainers.

Two conventional torsional moment diagrams according to DnV Manual [11] are shown in Fig. 36 /full line/ for the ship under consideration as well as corresponding torque intensities /dashed line/ obtained by differentiating. They correspond to the torsional load on the hull girder in waves for following /loadcase 1/ and for heading seas /loadcase 2/ for ship in the upright condition.

The ship hull idealization is shown in Fig. 37. The open part is assumed all over the loading part of the hull /hold no. 1, 2, 3, 4/. Bulky transverse deck strips are considered as warping restraining internal structure according to the principles described in Sec. 2. Cross section properties were therefore determined without transverse deck strips over the open part. The deckhouse was, however, included in the cross secion properties calculations.

To obtain the flexibility matrix and additional stresses /due to local bending of the warping restraining deck structure/ the deck frame analysis is to be performed. The frame idealization for foredeck as well as upper and lower deck is shown in Fig. 39.

The following calculation results are shown in Fig. 38 /from the top/: angle of rotation, warping, warping stresses /dashed line/ and total normal stresses /full line/ in the upper deck stringer.

Total normal stresses are calculated by adding local bending stresses, obtained from deck frame analysis, to primary warping stresses in the hull, computed by means of the above descibed program. As it can be noticed in Fig. 39 c and d the former /obtained as difference between full line and dashed line diagram/ are of the same order of magnitude as the latter.

To obtain actual values of stresses in the deck stringer additional stresses in warping restraining deck structure have to be determined through deck frame analysis. Such stresses can not be found when transverse deck strips are idealized as isolated beams, as it is the case in some conventional algorithms. It is probably the source of errors in the stress results described for instance in [7].

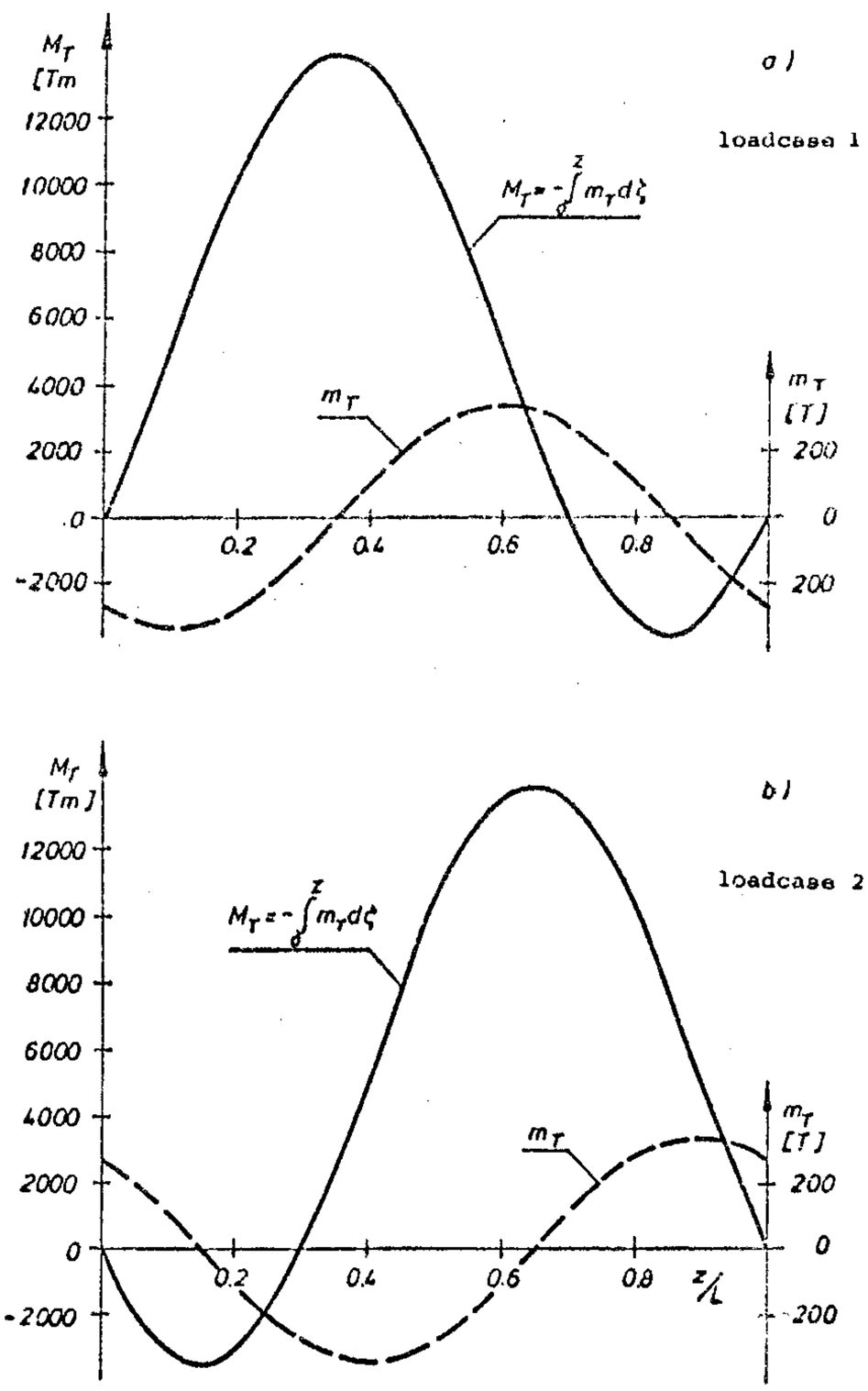

Fig. 36. Torsional load according to DnV Manual [11]

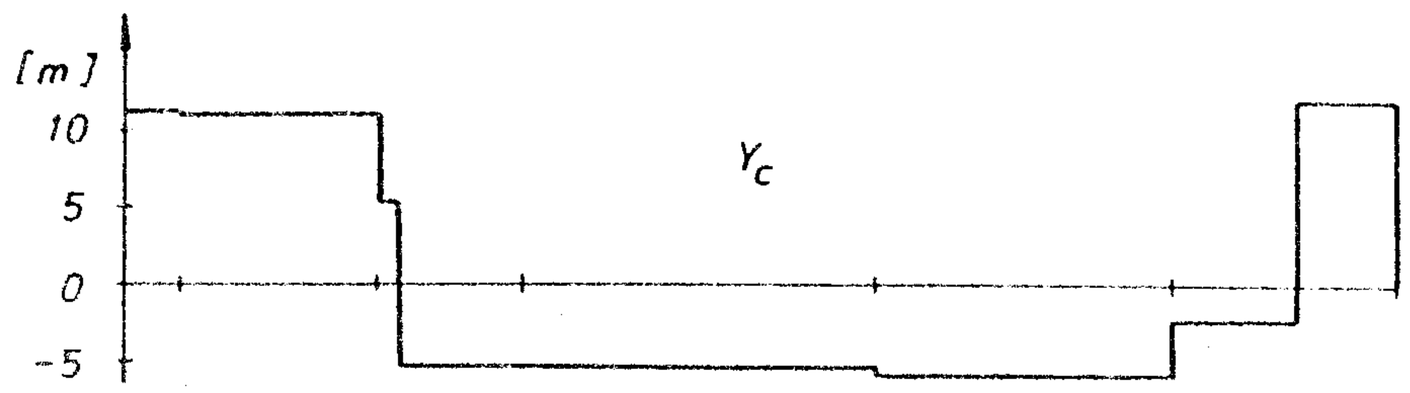

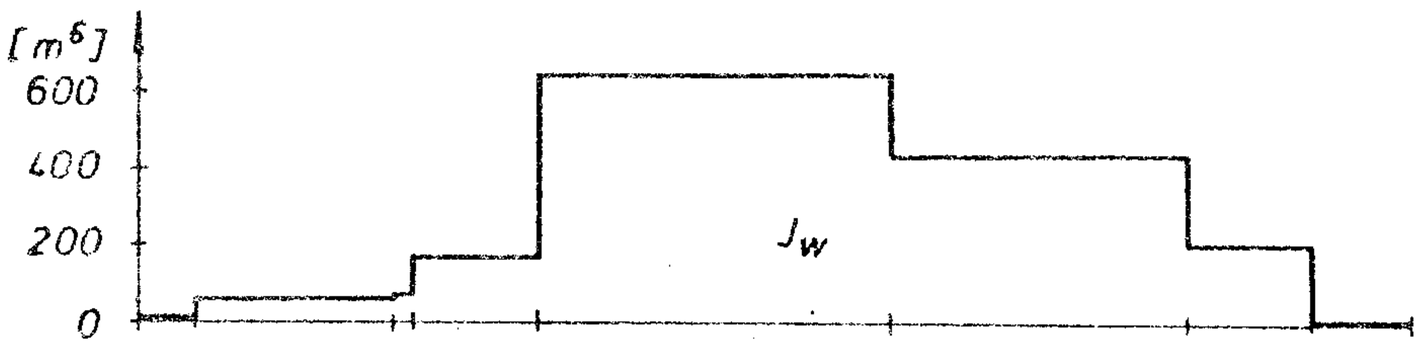

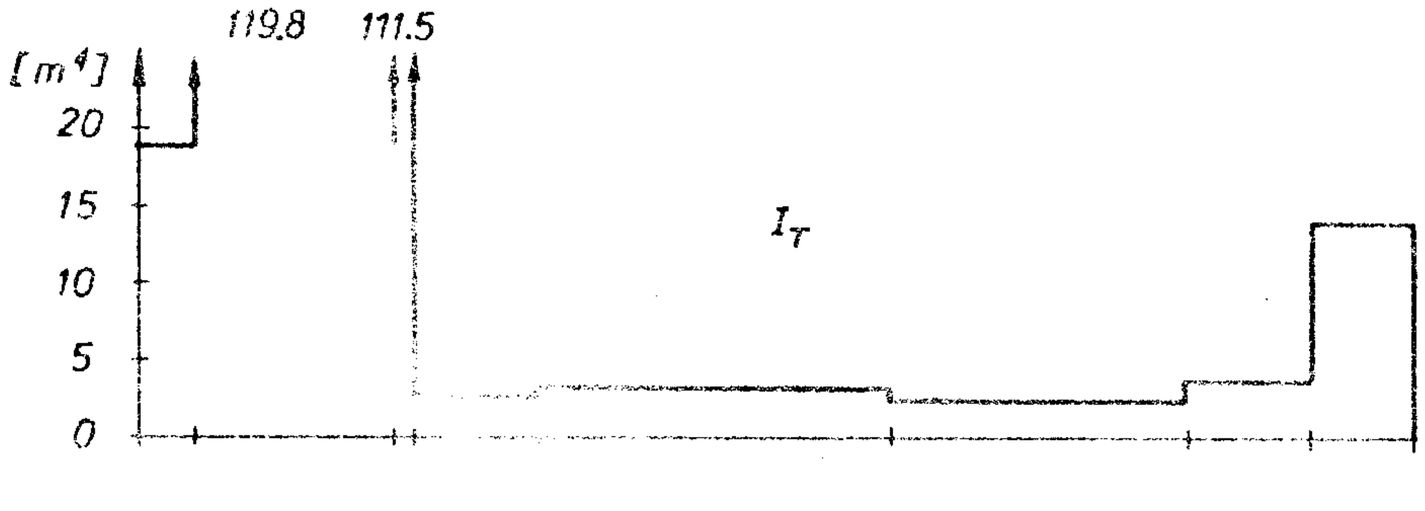

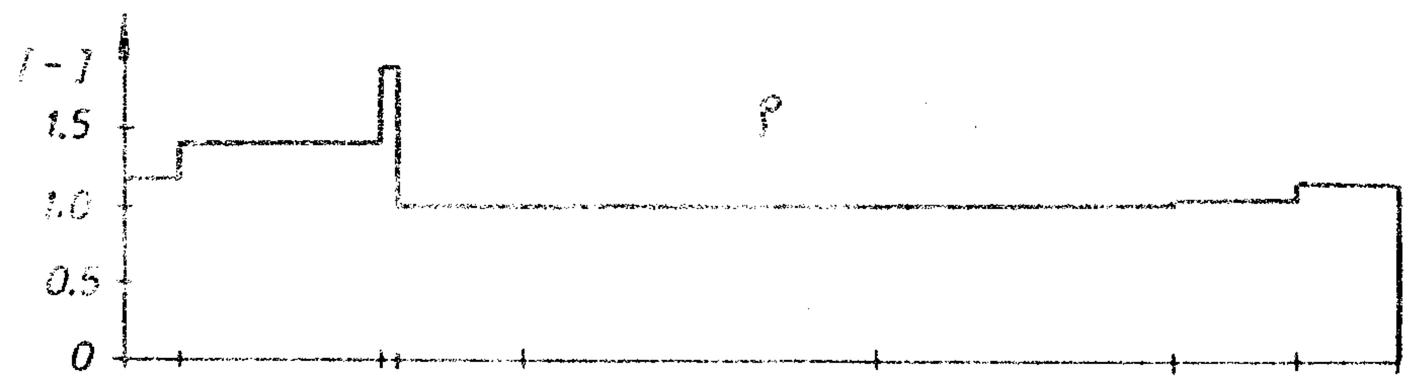

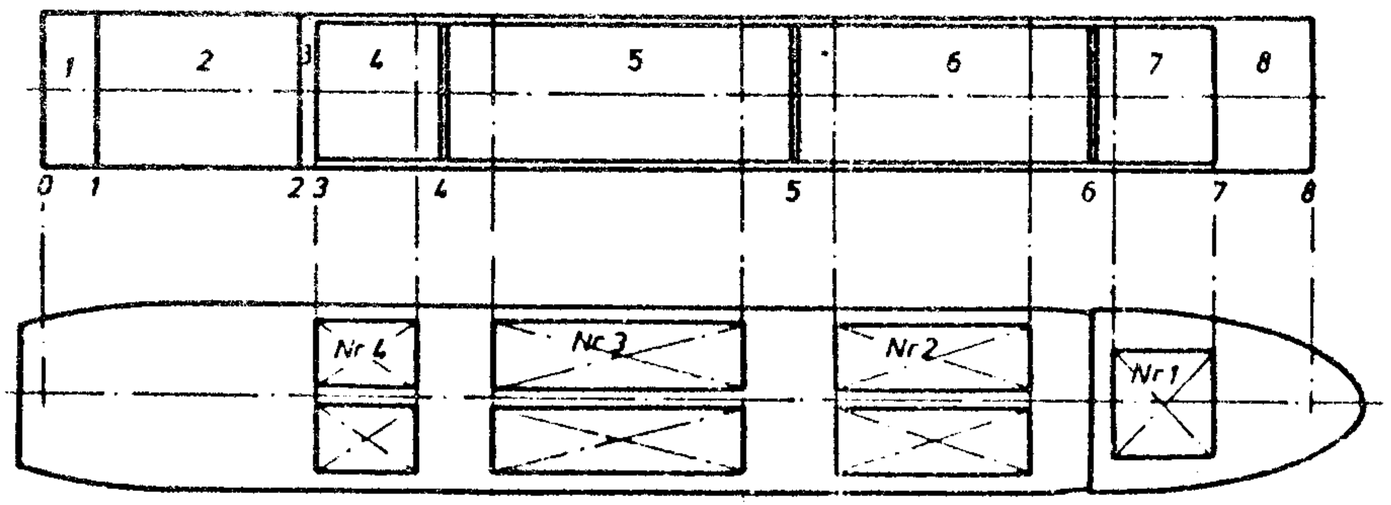

Fig. 37. A ship hull idealization and cross section properties distribution assumed

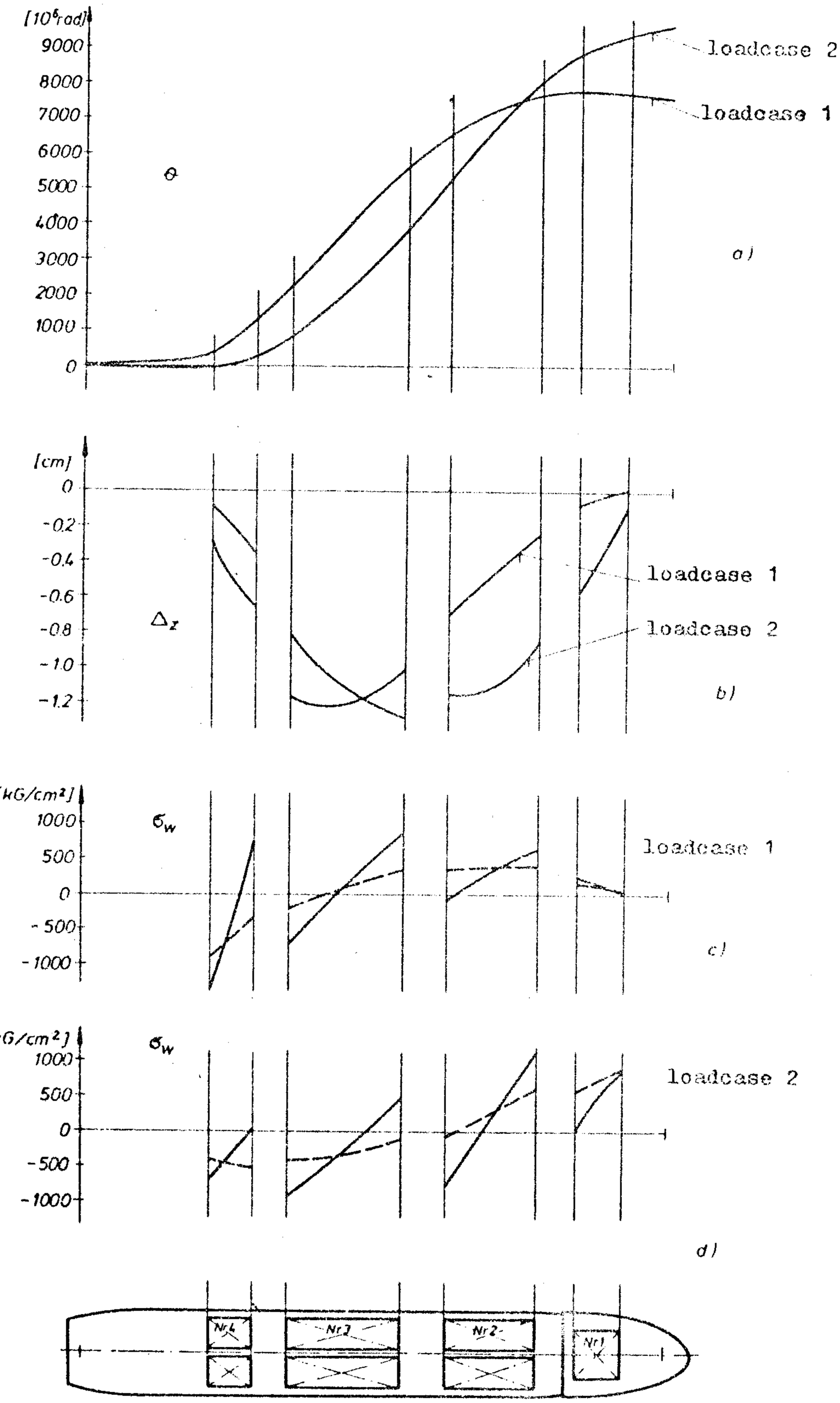

Fig. 38. Calculation results: Angle of rotation, warping, warping stresses /dashed line/ and total normal stresses /full line/ in the upper deck stringer

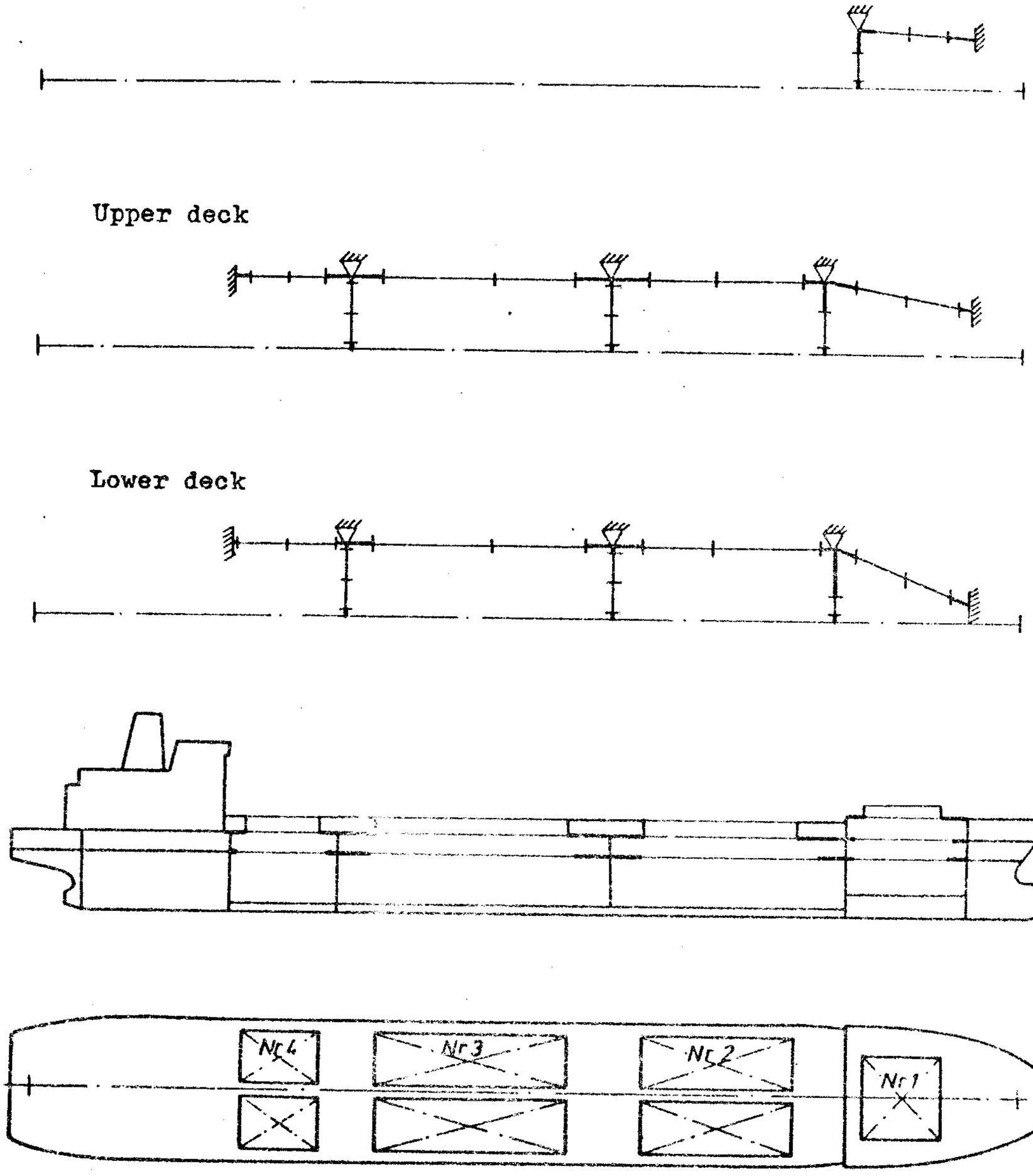

Fig. 39 A frame idealization of the ship decks

7. CONCLUSIONS

A significant improvement in the accuracy of results can be attained when the value of compatibility coefficient α according to /9/ is introduced at the junction of the open and closed hull parts. On the contrary, expression of the fictitious discontinuity at cross section between elements by introducing α determined according to /9/ leads to considerable inaccuracies. It is therefore recommended to put $\alpha = 1$ at these sections. Likewise, $\rho = 1$ should be assumed instead of the "exact" ρ value according to the formula given on page 11 when a beam with an open cross section is considered.

Making allowances for the coupling between horizontal bending and torsion according to the condition /10g/ introduced by Shimizu et al [4] leads to considerable discrepancies in comparsion with the results of FEM calculations in the case of high values of horizontal bending moment at junction section of the open and closed parts. Better results are in general obtained when coupling term in /10g/ is disregarded. The results of FEM calculations indicate, however, that a coupling between horizontal bending and torsion actually takes place. A significant improvement in the accuracy of results can be attained if the modification of condition /10g/ described on page 28 is introduced. As a rule, the appropriate results are better /or at least equivalent/ than those obtained after neglecting the second term in /10g/. Further researche is needed in this field.

To obtain actual values of stresses in a deck stringer additional stresses in warping restraining deck structure have to be determined through the deck plane frame analysis. Such stresses can not be obtained when transverse deck strips are idealized as isolated transverse beams restraining hull warping. The additional stresses are of the same order of magnitude as the primary warping stresses in the hull /at least in the case of bulky transverse deck strips/. Accuracy of results as dependent on the hull girder discretization as well as on the way the bulky transverse deck strips are idealized remains to be verified. It follows from [4], [7], [8] that comparatively coarse discretization suffices and transverse deck strips should be idealized as warping restraining internal structure rather than elements of a closed section of an appropriate hull girder segment.

ACKNOWLEDGEMENTS

The computer program described in the paper derives from an earlier one, originally developed in The Ship Design and Research Centre in cooperation with The Shipbuilding Computer Centre in Gdańsk and subsequently updated to take vertical and horizontal bending and shear into account. The earlier work is acknowledged as the root source for the present development.

The authors are grateful to colleagues in The Ship Structure Mechanics Division for their help and contribution to the paper. Example C was rendered accesible by Mr K. Tomaszewski.

BIBLIOGRAPHY

1. Kollbrunner C.F., Hajdin N.: Wölbkrafttorsion dünnwändiger Stäbe mit offenem Profil. Teil I. Mitteilungen der T.K.S.S.V. Heft 29. Verlag S.S.V. Zürich.
2. Kollbrunner C.F., Hajdin N.: Wölbkrafttorsion dünnwändiger Stäbe mit geschlossenem Profil. Mitteilungen der T.K.S.S.V. Heft 32. Verlag S.S.V. Zürich.
3. Haslum K., Tonnesen A.: An analysis of torsion in ship hulls. Europ. Shipbuild. 1972 no. 5/6.
4. Shimizu S., Yashima H.: Study of the longitudinal strength of ships with torsional and horizontal deformations. J.S.N.A. Japan. May 1974.
5. Instrukcja użytkowania programu TAW16J "Obliczanie wytrzymałości ogólnej kadłuba". 1979 maszyn. Centrum Techniki Okrętowej Gdańsk, nr RK-79/U-039.
6. Wekezer J.: Statyka belek cienkościennych o zmiennych przekrojach otwartych Rozprawy Inżynierskie /Engineering Transactions/. Warszawa 1976. T.24 z.1.
7. Seathre J.: Beregning av torsjonsspenninger i dekk ved hjelp av rammeprogram. Det norske Veritas. Forskningsavdelingen. Raport Nr 74-51-S.
8. Steneroth E.R., Ulfvarson A.Y.L.: The snaking of open ships. Int. Shipbuild. Progr.1976. Vol. 24, no.257.
9. Opracowanie metody analizy konstrukcji statków otwartych. Praca zbiorowa. Instytut Okrętowy Politechniki Gdańskiej. Zlecenie CTO nr 543/G-IV/72 Gdańsk 1973.
10. Bragazza G., Sani G.: Studio teorico dei fenomeni torsionali in navi a grandi aperture. Registro Italiano Navale. Boll. Tecnico n. 45 luglio 1971.
11. P. Lersbryggen, Ships´load and strength manual. Det norske Veritas. Feb. 1978.

APPENDIX I.

SUBMATRICES OF THE HULL GIRDER ELEMENT NO N TRANSFER MATRIX $\mathbb{F}_n$

$$\mathbb{K}_y(z) = \begin{bmatrix} 1 & \frac{z}{b^*} & \frac{EI^*_{yy}}{EI^{(n)}_{yy}} \cdot \frac{z^2}{2b^{*2}} & \frac{GA^*_y}{GA^{(n)}_y}\left(\frac{z}{b^*} - \frac{GA^{(n)}_y}{EI^{(n)}_{yy}}\frac{z^3}{6b^*}\right) \\ 0 & 1 & \frac{EI^*_{yy}}{EI^{(n)}_{yy}} \cdot \frac{z^2}{b^*} & -\frac{GA^*_y}{EI^{(n)}_{yy}}\frac{z^2}{2} \\ 0 & 0 & 1 & -\frac{GA^*_y}{EI^*_{yy}} b^* z \\ 0 & 0 & 0 & 1 \end{bmatrix}$$

$$\mathbb{K}_x(z) = \begin{bmatrix} 1 & \frac{z}{b^*} & \frac{EI^*_{xx}}{EI^{(n)}_{xx}} \cdot \frac{z^2}{2b^{*2}} & \frac{GA^*_x}{GA^{(n)}_x}\left(\frac{z}{b^*} - \frac{GA^{(n)}_x}{EI^{(n)}_{xx}}\frac{z^3}{6b^*}\right. \\ 0 & 1 & \frac{EI^*_{xx}}{EI^{(n)}_{xx}} \cdot \frac{z}{b^*} & -\frac{GA^*_x}{EI^{(n)}_{xx}} \cdot \frac{z^2}{2} \\ 0 & 0 & 1 & -\frac{GA^*_x}{EI^{(n)}_{xx}} b^* z \\ 0 & 0 & 0 & 1 \end{bmatrix}$$

$$\mathbb{K}_\varphi(z) = \begin{bmatrix} 1 & \frac{sh\,kz}{k\rho b^*} & \frac{GK^*}{GK^{(n)}}(1-ch\,kz) & \frac{GK^*}{GK^{(n)}}\left(\frac{z}{b^*} - \frac{sh\,kz}{k\rho b^*}\right) \\ 0 & ch\,kz & -\frac{GK^*}{GK^{(n)}} k\rho b^* sh\,kz & \frac{GK^*}{GK^{(n)}}(1-ch\,kz) \\ 0 & -\frac{GK^{(n)}}{GK^*}\frac{sh\,kz}{k\rho b^*} & ch\,kz & \frac{sh\,kz}{k\rho b^*} \\ 0 & 0 & 0 & 1 \end{bmatrix}$$

$$\mathbb{k}_y(z) = \begin{cases} 0 & dla \quad z \leqslant t_1 \\ \mathbb{k}_y(z-t_1) & dla \quad t_1 \leqslant z \leqslant t_2 \\ \mathbb{k}_y(z-t_1) - \mathbb{k}_y(z-t_2) & dla \quad t_2 \leqslant z \end{cases}$$

The same is valid for $\mathbb{k}_x(z)$ and $\mathbb{k}_\varphi(z)$ where

$$k = \sqrt{\frac{GK^{(n)}}{\rho E I^{(n)}_{\Omega\Omega}}}$$

$$\rho = \frac{I^{(n)}_{hh}}{I^{(n)}_{hh} - K^{(n)}}$$

$$\Delta p_y = p_{2y} - p_{1y}$$

$$\Delta p_x = p_{2x} - p_{1x}$$

$$\Delta m = m_2 - m_1$$

Abscissas t_1 and t_2 define position of a trapezoidal load applied to the considered element n /Fig. 3/.

$$\mathbb{k}_y(z-t_1) = \begin{bmatrix} \frac{(z-t_1)^4}{120 E I^{(n)}_{yy} b^*}\left(5p_{1y} + \frac{z-t_1}{t_2-t_1}\Delta p_y\right) - \frac{(z-t_1)^2}{6GA^{(n)}_y b^*}\left(3p_{1y} + \frac{z-t_1}{t_2-t_1}\Delta p_y\right) \\ \frac{(z-t_1)^3}{24 E I^{(n)}_{yy}}\left(4p_{1y} + \frac{z-t_1}{t_2-t_1}\Delta p_y\right) \\ \frac{b^*(z-t_1)^2}{6 E I^*_{yy}}\left(3p_{1y} + \frac{z-t_1}{t_2-t_1}\Delta p_y\right) \\ -\frac{z-t_1}{2GA^*_y}\left(2p_{1y} + \frac{z-t_1}{t_2-t_1}\Delta p_y\right) \end{bmatrix}$$

$$
\begin{aligned}
/\!/K_x(z-t_1) = \Bigg[& \frac{(z-t_1)^4}{120 EI^{(n)}_{xx} b^*}\left(5P_{1x} + \frac{z-t_1}{t_2-t_1}\Delta P_x\right) - \frac{(z-t_1)^2}{6GA^{(n)}_x b^*}\left(3P_{1x} + \frac{z-t_1}{t_2-t_1}\Delta P_x\right) \\
& \frac{(z-t_1)^3}{24 EI^{(n)}_{xx}}\left(4P_{1x} + \frac{z-t_1}{t_2-t_1}\Delta P_x\right) \\
& \frac{b^*(z-t_1)^2}{6 EI^*_{xx}}\left(3P_{1x} + \frac{z-t_1}{t_2-t_1}\Delta P_x\right) \\
& -\frac{z-t_1}{2GA^*_y}\left(2P_{1x} + \frac{z-t_1}{t_2-t_1}\Delta P_x\right) \Bigg]
\end{aligned}
$$

$$
\begin{aligned}
/\!/K_\varphi(z-t_1) = \Bigg[& -\frac{1}{GK^{(n)}}\left\langle m_1\left\{\frac{(z-t_1)^2}{2} + \frac{1}{k^2\rho}\left(1-chk(z-t_1)\right)\right\} + \frac{\Delta m}{t_2-t_1}\left\{\frac{(z-t_1)^3}{6} + \frac{1}{k^2\rho}\left(z-t_1 - \frac{1}{k}shk(z-t_1)\right)\right\}\right\rangle \\
& -\frac{b^*}{GK^{(n)}}\left\{m_1\left(z-t_1 - \frac{1}{k}shk(z-t_1)\right) + \frac{\Delta m}{t_2-t_1}\left[\frac{(z-t_1)^2}{2} + \frac{1}{k^2}\left(1-chk(z-t_1)\right)\right]\right\} \\
& -\frac{1}{k^2\rho GK^*}\left\{m_1\left(chk(z-t_1)-1\right) + \frac{\Delta m}{t_2-t_1}\left(\frac{1}{k}shk(z-t_1) - (z-t_1)\right)\right\} \\
& -\frac{b^*}{GK^*}\left\{m_1(z-t_1) + \frac{\Delta m}{t_2-t_1}\frac{(z-t_1)^2}{2}\right\} \Bigg]
\end{aligned}
$$

APPENDIX II.

COMPATIBILITY AND EQUILIBRIUM CONDITIONS FOR THE CROSS SECTION N BETWEEN ELEMENTS

Horizontal displacements ξ_p of the point P /Fig.2/ depend on horizontal displacement ξ of the shear centre D according to the formula

$$\xi_p = \xi + e\varphi$$

From the condition of equal horizontal displacements of the point P at the left and right hand side of the section n between elements it follows

$$\xi_n^L + \varphi_n e_n = \xi_n^R + \varphi_n e_{n+1}$$

and

$$\xi_n^R = \xi_n^L - \varphi_n (e_{n+1} - e_n)$$

where ξ_n^L , ξ_n^R means the shear centre displacement of the left and right hand side of the section n

e_n , e_{n+1} means the shear centre ordinate of the element at the left and right hand side of the section n

"Bimoment" in relation to the pole at point P is determined according to the definition

$$M_{\omega P} = \int_F \sigma \omega_p dF$$

It can be proved that /at least for an open cross section/ the following relation holds

$$M_{\omega P} = - EI_{x\omega P} \xi''' - EI_{\omega\omega P} \varphi''$$

After having applied the transformation rule for sectorial coordinates / Ω denotes sectorial coordinates in relation to the shear centre D/

$$\omega_p = \Omega - ex$$

$$I_{x\omega P} = \int_F \omega_p x dF = - e I_{xx}$$

$$I_{\omega\omega P} = \int \omega_p \omega_p dF = I_{\Omega\Omega} + e^2 I_{xx}$$

and the relation for horizontal displacement derivatives

$$\xi_P'' = \xi'' + e\varphi''$$

the following relations can be derived

$$M_{\omega P} = M_\Omega + e M_x$$

where

$$M_\Omega = \int_F \sigma \Omega \, dF = -EI_{\Omega\Omega}\varphi''$$

$$M_x = \int_F \sigma x \, dF = EI_{xx}\xi''$$

From the condition of equal "bimoments" $M_{\omega P}$ at the left and right hand side of the section n between elements it follows

$$M_{\Omega,n}^L + e_n M_{x,n} = M_{\Omega,n}^R + e_{n+1} M_{x,n}$$

where from

$$M_{\Omega,n}^R = M_{\Omega,n}^L - (e_{n+1} - e_n) M_{x,n}$$

where M_Ω^L and M_Ω^R denote bimoments in relation to the pole at the shear centre of the element to the left and right of the section n between elements, $M_{x,n}$ means a horizontal bending moment in the section.

A torsional moment in relation to the point P can be connected with the torsional moment in relation to the shear centre D

$$T_p = T - e Q_x$$

assuming the convention shown in Fig. 2. From the condition of equal torsional moments T_p at both sides of the section n it follows

$$T_n^L - e_n Q_{x,n} = T_n^R - e_{n+1} Q_{x,n}$$

where from

$$T_n^R = T_n^L + Q_{x,n}(e_{n+1} - e_n)$$

where T_n^L and T_n^R denote the torsional moment in relation to the shear centre of the element at the left and right hand side of the section n, $Q_{x,n}$ means horizontal shear force in section n.

WYDAWCA: Centrum Techniki Okrętowej – BOINTE PO
Gdańsk, ul. Wały Piastowskie 1

Powielono w CTO, nakład 160 egz., zam. nr 6434 R.